TAMPERE UNIVERSITY OF TECHNOLOGY

CLEEN
Cluster for Energy and Environment

# THERMO-CATALYTIC DECOMPOSITION OF METHANE:
## ANNUAL REPORT

Markus Fager-Pintilä
Tampere University of Technology

Cleen CCSP-program,
FP II, WP 2.5.2
Tampere 2013

## ABSTRACT

Concerns about the rising carbon dioxide concentration in the atmosphere and its possible negative effects on life on Earth have forced governments to take actions. Many new technologies are being investigated in order to find more economically and environmentally friendly and energy-efficient methods, which could replace the conventional technologies. The power-generation industry, in particular, has shown interest, as currently the majority of electricity is produced from fossil fuels.

Cleen Oy launched a carbon capture and storage –program (CCSP) in 2011, to find and evaluate novel ways to mitigate anthropogenic emissions to the atmosphere. As a part of the program, Tampere University of Technology has conducted research on a pre-combustion carbon capturing method 'Thermo-catalytic Decomposition of Methane'. Research started as Master's Thesis and is planned to continue throughout the planned project span, 2011-2015.

During the funding period I, literature and patent review was made. Also a set of laboratory experiments was designed and conducted. Main finding from the FP I was that the reaction does take place in conditions possible to theoretically create in a larger scale. However, by optimizing both the process parameters and the catalyst used the reaction conversion percentage could possibly be higher in less severe surroundings. It was acknowledged, that as a hydrogen production method, TDM should economically overcome the current technology, steam-methane reformation,

During the funding period II, experiments were widened to cover different types of catalysts used in reaction. One goal was to find a cheap, abundant catalyst and e.g. quartz sand and biomass-based char was tested. The results were that either had very little effect on the decomposition reaction. In addition, in the high temperature required to obtain a reasonable reaction conversion rate, bio char completely lost its active surface area possibly due to the ash component melting. The commercial carbon black used already during FP I tests was further evaluated. Results indicate the high surface area is a critical requirement in order to reach even a moderate decomposition rate.

The results and experiences obtained during the FP I and II lead the author to suggest taking the metal catalysts, previously out of the scope, into the account. It would offer comparison data to make further conclusions about the catalyst requirements and decomposition efficiency, i.e. offer more tools to conduct techno-economical analysis.

# TABLE OF CONTENTS

# ABBREVIATIONS AND NOTATION

| Symbol | Units | Definition |
|---|---|---|
| $a$ | - | chemical activity |
| $a$ | - | conversion |
| $A$ | | pre-exponential factor; frequency factor |
| $C$ | mol $m^{-3}$ | concentration |
| $C_{pm}$ | J $mol^{-1}$ $K^{-1}$ | molar specific heat capacity |
| $E_a$ | J $mol^{-1}$ | activation energy |
| $\Delta H_f$ | J $mol^{-1}$ | formation enthalpy |
| $\Delta H_r$ | J $mol^{-1}$ | reaction enthalpy |
| $H_m$ | J $mol^{-1}$ | molar sensible enthalpy |
| $k$ | | reaction rate coefficient; rate constant |
| $K$ | | chemical equilibrium constant |
| $K_p$ | | chemical equilibrium constant in terms of pressure |
| $M$ | g $mol^{-1}$ | molar mass |
| $m$ | kg | mass |
| $\dot{m}$ | kg $s^{-1}$ | mass flow rate |
| $n$ | mol | mole mass |
| $n$ | - | reaction order |
| $\dot{n}$ | mol $s^{-1}$ | molar flow rate |
| $p$ | Pa | pressure |
| $Q$ | J $mol^{-1}$ | molar heat |
| $r$ | | reaction rate |
| $T$ | K | temperature |
| $V$ | $m^3$ | volume |
| $VHSV$ | 1/h | volume hourly space velocity |
| $\dot{V}$ | $m^3$ $s^{-1}$ | volumetric flow rate |
| $x$ | - | volumetric fraction |

| Greek symbols | Units | Definition |
|---|---|---|
| $\rho$ | kg $m^{-3}$ | density |
| $\tau$ | s | residence time |
| $\chi$ | - | conversion |

| Constants | Units | Definition |
|---|---|---|
| $R_u$ | J $mol^{-1}$ $K^{-1}$ | universal gas constant, 8.314 J $mol^{-1}$ $K^{-1}$ |

| Subscripts | Definition |
|---|---|
| *bed* | reactor bed condition |
| *C* | carbon |
| *i* | species i |
| *in* | reactor inlet condition |
| *inlet* | reactor inlet condition |
| *p* | pressure |

**Abbreviations**

| | |
|---|---|
| **AC** | Activated carbon |
| **BET** | Brunauer-Emmett-Teller –surface area |
| **CB** | Carbon black |
| **CCS** | Carbon capture and storage |
| **FP** | Funding period |
| **LHV** | Lower heating value |
| **STP** | Standard temperature and pressure |
| **TDM** | Thermo-catalytic decomposition of methane |

# 1 INTRODUCTION

The aim of this research is to examine the potential of thermocatalytic decomposition of methane (TDM) as a method to reduce carbon dioxide emissions in natural gas combustion. The only reaction products are gaseous hydrogen and solid carbon, which both also have a potential aftermarket thus increasing the interest. Methane is the main component of natural gas, which is used in Finland mainly for the production of energy. As natural gas is mostly used in small units, the post-combustion sequestration and storage of $CO_2$ with the conventional methods is both impractical and expensive. An alternative approach is to separate and capture the carbon before combustion. To become economically attractive hydrogen production method, TDM must have both lower costs and lower emissions than the current *de facto*-process, steam reformation.

Although the carbon dioxide capture and storage (CCS) is globally a hot topic, concrete actions have been quite modest. A few pilot plants have been launched, but many of them have also been shut down or cancelled due to various reasons. No consensus on storaging the captured $CO_2$ has been reached, and to be realistic, it might still take even another twenty years to have a functioning CCS-infrastructure.

TDM can be seen as a first-generation method to lower the $CO_2$ emissions in natural gas use, and help the industry to meet the stricter emission limits in the years to come. It can buy the valuable time needed to come up with novel sustainable solutions without forcing the plants to shut down.

# 2 REACTION EQUILIBRIUM AND CONVERSION

## 2.1 In general

In general a chemical reaction can be expressed as follows

$$jA + kB \leftrightarrow lC + mD, \tag{2.1}$$

where upper case letters A and B represent the reactants and C and D the products of reaction. Lower case letters denote the stoichiometric reaction coefficients.

The equilibrium constant, K, for reaction, is calculated with the following formula

$$K = \frac{(a_C)^l (a_D)^m}{(a_A)^j (a_B)^k}, \tag{2.2}$$

where $a_i$ denotes the chemical activity of a substance. The exponents for the substance activities are the corresponding stoichiometric coefficients.

The activity can be expressed in terms of pressure, when it becomes

$$a_i = \frac{p_i}{p_{ref}}, \tag{2.3}$$

where $p_i$ represents the partial pressure of a gas, and $p_{ref}$ the reference pressure, the value of which is usually 1 atmosphere (1 atm). In addition, it has to be remembered that in heterogeneous reactions the activity of non-gaseous substances is unity.

From the ideal gas law it can be shown, that the pressure fraction equals the mole fraction of a substance.

$$pV = nR_u T \tag{2.4}$$

For component $i$ in a gas mixture

$$p_i V = n_i R_u T \tag{2.5}$$

$$n_i = \frac{p_i V}{R_u T} \tag{2.6}$$

For the total amount:

$$p_{tot}V = n_{tot}R_uT \tag{2.7}$$

$$n_{tot} = \frac{p_{tot}V}{R_uT} \tag{2.8}$$

Mole fraction for the species $i$ is

$$x_i = \frac{n_i}{n_{tot}} \tag{2.9}$$

Amounts of substances can be replaced by:

$$x_i = \frac{\frac{p_iV}{R_uT}}{\frac{p_{tot}V}{R_uT}} \tag{2.10}$$

Which can be simplified,

$$x_i = \frac{p_i}{p_{tot}}. \tag{2.11}$$

## 2.2 For TDM

The stoichiometric equation for thermocatalytic decomposition of methane taking place in a nitrogen atmosphere is

$$A \cdot CH_4(g) + B \cdot N_2(g) \leftrightarrow A \cdot C(s) + 2A \cdot H_2(g) + B \cdot N_2(g), \tag{2.12}$$

where A and B are the stoichiometric coefficients. Initial methane concentration (mole fraction) based on the Equation 2.12 is as follows:

$$mole\ fraction\ of\ methane = \frac{A}{A + B}. \tag{2.13}$$

By using the common notation $x$ for mole fraction and by replacing the stoichiometric coefficients with the amounts of the substances Equation 4.2 becomes

$$x_{CH_4,0} = \frac{n_{CH_4,0}}{n_{CH_4,0} + n_{N_2}}. \tag{2.14}$$

Equation 2.14 is solved further in terms of nitrogen concentration:

$$x_{CH_4,0}\left(n_{CH_4,0} + n_{N_2}\right) = n_{CH_4,0}, \quad (2.15)$$

$$x_{CH_4,0}n_{CH_4,0} + x_{CH_4,0}n_{N_2} = n_{CH_4,0}, \quad (2.16)$$

$$x_{CH_4,0}n_{N_2} = n_{CH_4,0} - x_{CH_4,0}n_{CH_4,0}, \quad (2.17)$$

$$n_{N_2} = n_{CH_4,0}\frac{\left(1 - x_{CH_4,0}\right)}{x_{CH_4,0}}. \quad (2.18)$$

It is convenient to use one mole of $CH_4$ ($n_{CH_4,0} = 1\,mol$) as a base, thus reaction Equation 2.12 becomes

$$1CH_4(g) + \frac{\left(1 - x_{CH_4,0}\right)}{x_{CH_4,0}}N_2(g) \leftrightarrow 1C(s) + 2H_2(g) + \frac{\left(1 - x_{CH_4,0}\right)}{x_{CH_4,0}}N_2(g), \quad (2.19)$$

and for simplicity, $B_1 = \frac{\left(1-x_{CH_4,0}\right)}{x_{CH_4,0}}$.

Table 2.1 shows the reaction equation coefficients both in the initial and in the equilibrium condition. Symbol $a$ denotes conversion and is discussed in Section 0.

***Table 2.1.*** *Reaction equation coefficients.*

| | 1 **$CH_4$** + $B_1$ $N_2$ ↔ **C(s)** + **$2H_2$ (g)** + $B_1$ $N_2$ | | | | | | |
|---|---|---|---|---|---|---|---|
| | | | | | | **sum** | |
| **start** | 1 | $B_1$ | 0 | 0 | 0 | 1+ $B_1$ | mol |
| **equilibrium** | 1-a | 0 | a | 2a | $B_1$ | 1+2a+ $B_1$ | mol |
| | | | | | gas phase | 1+a+ $B_1$ | mol |

### 2.2.1 Equilibrium

With the method described in Section 2.1, the equilibrium constant for methane decomposition reaction becomes

$$K = \frac{(a_C)^1\left(a_{H_2}\right)^2}{\left(a_{CH_4}\right)^1} \quad (2.20)$$

When the activities are replaced with the pressure ratio from Equation 3.11 (and remembering that $a_C$=1), the value of the equilibrium constant $K_p$ is normally given by

$$K_p = \frac{1 \cdot \left(\frac{p_{H_2}}{p_{ref}}\right)^2}{\left(\frac{p_{CH_4}}{p_{ref}}\right)^1} \tag{2.21}$$

Equation 3.13 can be further modified to include the effect of the operating pressure, by expanding the equation to include the total operating pressure:

$$K_p = \frac{\left(\frac{p_{H_2}}{p_{tot}} \cdot \frac{p_{tot}}{p_{ref}}\right)^2}{\left(\frac{p_{CH_4}}{p_{tot}} \cdot \frac{p_{tot}}{p_{ref}}\right)} \tag{2.22}$$

Pressure ratios can be replaced by the mole fractions, as follows

$$K_p = \frac{\left(x_{H_2} \cdot \frac{p_{tot}}{p_{ref}}\right)^2}{\left(x_{CH_4} \cdot \frac{p_{tot}}{p_{ref}}\right)} \tag{2.23}$$

$$K_p = \frac{{x_{H_2}}^2}{x_{CH_4}} \frac{p_{tot}}{p_{ref}} \tag{2.24}$$

We can formulate the mole fractions based on Table 2.1 as follows

$$x_{H_2} = \frac{2a}{1 + \mathbf{2}a + B_1} \tag{2.25}$$

$$x_{CH_4} = \frac{1 - a}{1 + \mathbf{2}a + B_1} \tag{2.26}$$

$$x_C = \frac{a}{1 + \mathbf{2}a + B_1} \tag{2.27}$$

By substituting the hydrogen and methane mole fractions, Equation *2.24* becomes

$$K_p = \frac{\left(\frac{2a}{1 + \mathbf{2}a + B_1}\right)^2}{\frac{1 - a}{1 + \mathbf{2}a + B_1}} \frac{p_{tot}}{p_{ref}} \tag{2.28}$$

$$K_p = \frac{(2a)^2}{(1 - a)(1 + \mathbf{2}a + B_1)} \frac{p_{tot}}{p_{ref}} \tag{2.29}$$

$$K_p = \frac{4a^2}{(1 + a - 2a^2)} \frac{p_{tot}}{p_{ref}} \tag{2.30}$$

By using the common denotion $\chi$ for conversion we get

$$K_p = \frac{4{\chi_{th}}^2}{\left(1 + \chi_{th} - 2{\chi_{th}}^2\right)} \frac{p_{tot}}{p_{ref}}, \tag{2.31}$$

where subscript $th$ emphasizes that Equation 2.31 doesn't take into account the fact that catalyst is present, but is merely for thermal decomposition. Conversion is then only a function of temperature and pressure.

Although the equilibrium constant relates to non-ideal gases, at close to atmospheric pressures the difference is negligible. It must be remembered, that the equilibrium calculations do not take into account in any way the contribution of the catalyst to the reaction. That is to say, the reaction kinetics, i.e. the rate at which the reactions take place, have to be determined experimentally. They vary considerably depending on the catalyst used so that fresh experiments have to be undertaken every time a new catalyst is to be used.

In the literature, the equilibrium constant for the reaction is usually expressed in terms of methane formation, thus after obtaining the constant values for the formation reaction, the complementary ones are used. The logarithmic value of the equilibrium constant versus temperature is plotted in Figure 2.1.

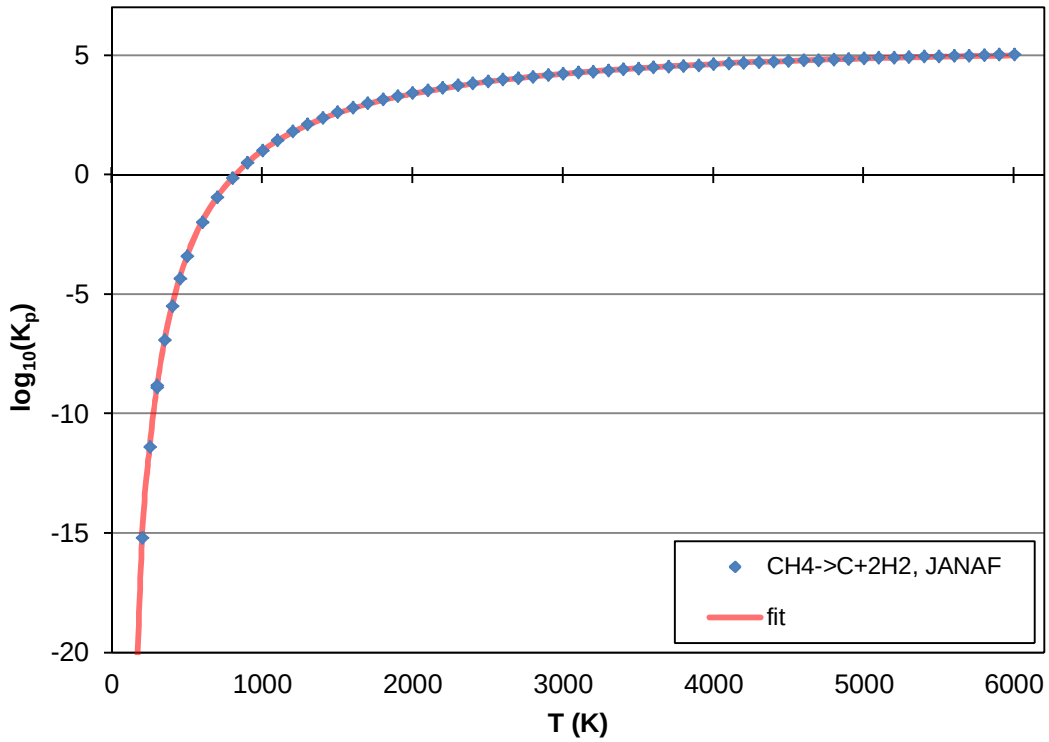


***Figure 2.1.*** *The logarithmic value of the equilibrium constant for methane thermal decomposition reaction versus the temperature.*

The fit shown in Figure 2.1 was constructed using the equilibrium constant tables, with the help of mathematical software, MatLab. The fit correlation is of the form

$$log_{10}[K_p(T)] = A \cdot \frac{\ln(B \cdot T)}{T} + B \cdot \ln(T) + \frac{C}{T} + D \cdot T + E, \tag{2.32}$$

where the constants are as follows:

A = -290.2
B = 0.5561
C = -2623
D = $-1.266 \cdot 10^{-4}$
E = 1.749.

The higher the value of $K_p$, the more the balance of the reaction moves towards the products. The figure in Appendix B shows that the temperature is an essential parameter in achieving a satisfactory level of decomposition. It is important to understand that the size of $K_p$ and the time required to reach equilibrium are not directly related.

Figure 2.2 illustrates the equilibrium mole fractions of the substances as a function of the temperature in TDM reaction at the atmospheric pressure.

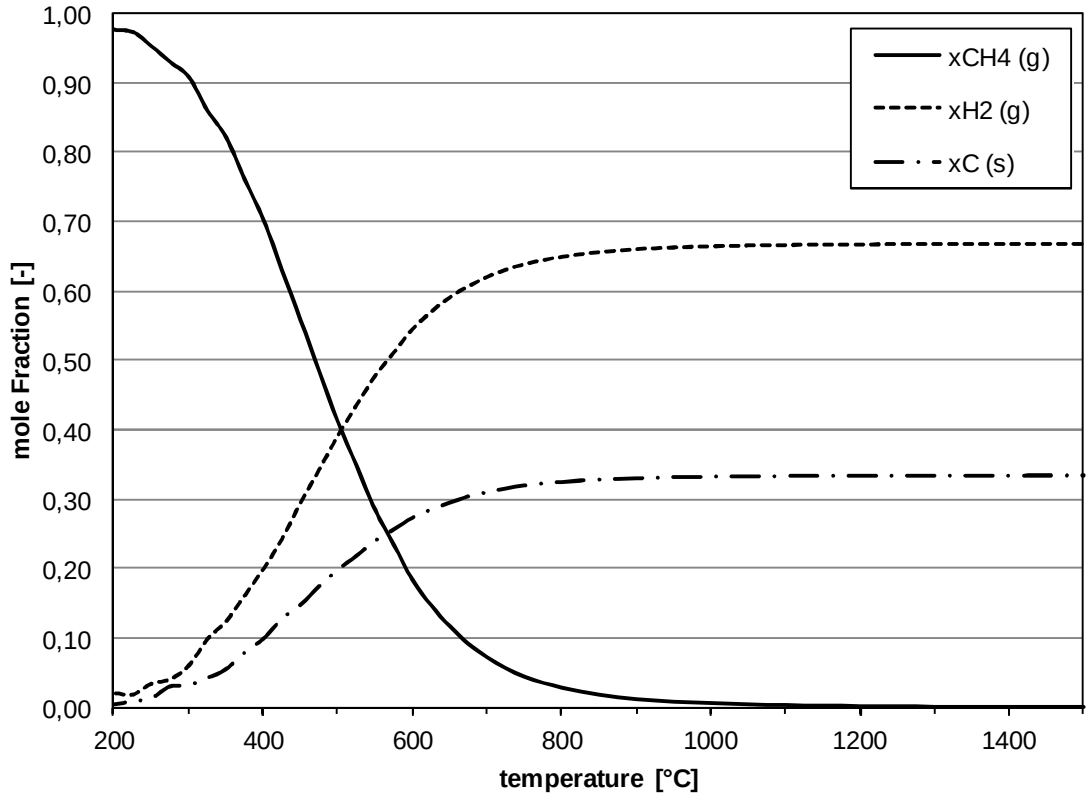


***Figure 2.2.*** *Equilibrium concentrations of reactant (methane) and reaction products (hydrogen and carbon) as functions of temperature.*

Comparison to the results obtained in the experiments is done in Section 7.4.

### 2.2.2 Conversion calculations

Based on the Table 2.1, methane mole fraction in gaseous phase is now

$$x_{CH_4} = \frac{1 - a}{1 + a + B_1}. \tag{2.33}$$

Solving Equation 2.33 in terms of $a$ gives

$$x_{CH_4}(1 + a + B_1) = 1 - a, \tag{2.34}$$

$$x_{CH_4} + ax_{CH_4} + B_1 x_{CH_4} = 1 - a, \tag{2.35}$$

$$ax_{CH_4} + a = 1 - x_{CH_4} - B_1 x_{CH_4} \tag{2.36}$$

$$a(1 + x_{CH_4}) = 1 - x_{CH_4}(1 + B_1) \tag{2.37}$$

$$a = \frac{1 - x_{CH_4}(1 + B_1)}{1 + x_{CH_4}} \tag{2.38}$$

$$a = \frac{1 - x_{CH_4}\left[1 + \frac{(1 - x_{CH_4,0})}{x_{CH_4,0}}\right]}{1 + x_{CH_4}}. \tag{2.39}$$

Similarly, equation for the conversion can be formulated starting with the hydrogen mole fraction, when it becomes

$$a = \frac{x_{H_2}\left[1 + \frac{(1 - x_{CH_4,0})}{x_{CH_4,0}}\right]}{2 - x_{H_2}} \tag{2.40}$$

Equations 2.39 and 2.40 give the conversion for any atmosphere. The special case is, when only methane stream is present, $x_{CH_4,0}$ = 100%:

$$a = \frac{1 - x_{CH_4}\left[1 + \frac{(1 - 1)}{1}\right]}{1 + x_{CH_4}} \tag{2.41}$$

$$a = \frac{1 - x_{CH_4}(1 + 0)}{1 + x_{CH_4}} \tag{2.42}$$

$$a = \frac{1 - x_{CH_4}}{1 + x_{CH_4}}. \tag{2.43}$$

When conversion is formulated with hydrogen concentration, and with 100% methane atmosphere, Equation 2.40 becomes

$$a = \frac{x_{H_2}}{2 - x_{H_2}}. \tag{2.44}$$

Equations 2.44 and 2.45 are common in research reports (e.g. Abbas & Daud, 2010).

# 3 ENERGY BALANCE CONSTRAINT

## 3.1 On reaction enthalpy

The chemical reaction is

$$CH_4(g) \leftrightarrow C(s) + 2H_2(g). \tag{3.1}$$

The reaction is endothermic, which means that it requires energy in order for it to take place. The formation enthalpy value $\Delta H_f$ for methane is usually ~ -75 MJ/kmol. Thus deformation enthalpy has the complement value, ~75 MJ/kmol. Formation enthalpy is given in standard temperature and pressure (STP: T=25 °C; p=101,325 Pa).

The reaction enthalpy $\Delta H_r$ is the difference between the enthalpies of the products and the reactants, but in this case all other substances present are elements for which the formation enthalpy is zero (0). Thus the reaction enthalpy equals the methane deformation enthalpy. It is a temperature dependent quantity, and its values are tabulated in thermo chemical databases. Figure 3.1 shows a graphic representation of some tabulated values, as well as the values used in Muradov's calculations. Interestingly, they seem to somewhat differ from all the other ones. Fit for calculation is introduced in Appendix C.

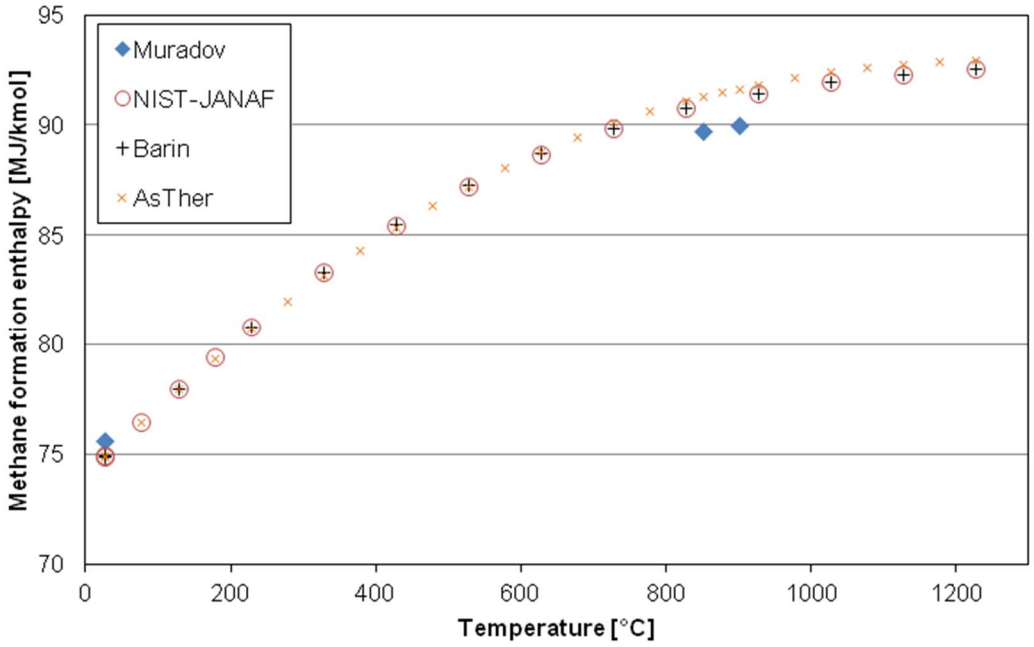


***Figure 3.1.*** *Methane formation enthalpies versus temperature, plotted from different sources.*

## 3.2 Energy to support the reaction

Several ways of producing the heat necessary to drive the reaction are reported in the literature. These can be divided roughly into two categories: heat sources that are based on the material streams essentially attached to TDM reaction, and sources that are independent of TDM. A division could also be made according to whether the heat input is direct or indirect. This becomes an option when the catalyst particles are circulated to a separate regeneration reactor, where they could be heated and carrying the energy necessary to drive the reaction in the decomposition reactor. Overall energy balance for the reaction is done here, assuming both the reactants and the products are in the reference state (STP).

***Table 3.1.*** *Net calorific heating values (LHV) from selected combustion reactions.*

| combustion reaction | $Q_m$ | $Q_M$ | $Q_V$ |
|---|---|---|---|
| | MJ/kg | MJ/kmol | MJ/m$^3$ |
| $CH_4 + 2O_2 \rightarrow CO_2 + 2H_2O$ | 50.05 | 802.93 | 35.82 |
| $H_2 + ½\ O_2 \rightarrow H_2O_{vap}$ | 120.00 | 241.92 | 10.79 |
| $C + O_2 \rightarrow CO_2$ | 32.80 | 393.96 | |

With the values obtained from the Table 3.1, following energy balance can be made.

***Table 3.2.*** *Energy balance for the TDM reaction and the energy balance distribution.*

For stoichiometric reaction: 1 $CH_4$ = 1 C(s)+ 2 $H_2$

| | | | | | | | | |
|---|---|---|---|---|---|---|---|---|
| $Q_{reactants}$ | 803 | | | | | | 803 | MJ/kmol |
| $\Delta h_f = \Delta H_r$ | 74.9 | (T= | 25 | °C) | | + | 75 | MJ/kmol |
| $Q_{input}$ | | | | | | = | 878 | MJ/kmol |
| $Q_{products}$ | | | 394 | | 484 | | -878 | MJ/kmol |
| | | | | | | = | 0 | MJ/kmol |

**Process stream heat / heat input: $Q_i$ / $Q_{input}$**

| | |
|---|---|
| $\Delta H_r$ | 8.53 % |
| $Q_{CH4}$ | 91.5 % |
| $Q_{H2}$ | 44.9 % |
| $Q_C$ | 55.1 % |

**Fraction of process stream heat to support the reaction enthalpy: $\Delta H_r$ / $Q_i$**

| | |
|---|---|
| $x_{CH4}$ | 9.3 % |
| $x_{H2}$ | 15.5 % |
| $x_C$ | 19.0 % |

A few conclusions can be drawn with the help of the Table 3.2: Formation enthalpy requires less than 10% of the input heat; more than 50% of the input heat is in the form

of a carbon; approximately 10% of the input methane would be required to support the reaction enthalpy.

## 3.3 Energy required

$$energy\ required\ = \\ energy\ consumed\ by\ reaction\ + \\ heating\ the\ feedstock\ to\ desired\ temperature$$

Thus we have

$$\dot{Q}\ =\ \chi\dot{n}_{inlet}\Delta H_r\ +\ \dot{n}_{inlet}C_{pm,CH_4}\left(T_{bed}-T_{CH_4,in}\right), \tag{3.2}$$

where $\chi$ is the methane conversion percentage and $C_{pm,CH_4}$ methane molar heat capacity. As heat capacity is a temperature dependent quantity as well, some average value should be used. It is actually more convenient to use sensible enthalpy values, $H_{m,i}$. Now Equation 3.2 becomes

$$\dot{Q}\ =\ \chi\dot{n}_{inlet}\Delta H_r\ +\ \dot{n}_{inlet}[H_{m,CH_4}(T_{bed})-H_{m,CH_4}(T_{in})] \tag{3.3}$$

In case diluting gas is used (most likely $N_2$), that has to be taken into account:

$$\begin{aligned}&\dot{Q}\ = \\ &\chi\cdot x_{CH_4,0}\dot{n}_{inlet}\Delta H_r+ \\ &x_{CH_4,0}\dot{n}_{inlet}\left[H_{m,CH_4}(T_{bed})-H_{m,CH_4}(T_{in})\right]+ \\ &x_{N_2}\dot{n}_{inlet}\left[H_{m,N_2}(T_{bed})-H_{m,N_2}(T_{in})\right]\end{aligned} \tag{3.4}$$

As the conversion reduces over time, it is taken into consideration by implying the conversion correlation 2.39:

$$\chi\ =\ \frac{1-x_{CH_4}\left[1+\frac{\left(1-x_{CH_4,0}\right)}{x_{CH_4,0}}\right]}{1+x_{CH_4}} \tag{3.5}$$

Now Equation 3.4 becomes

$$\dot{Q} = \dot{n}_{inlet}\{\frac{1-x_{CH_4}\left[1+\frac{(1-x_{CH_4,0})}{x_{CH_4,0}}\right]}{1+x_{CH_4}} \cdot x_{CH_4,0}\Delta H_r + x_{CH_4,0}\left[H_{m,CH_4}(T_{bed}) - H_{m,CH_4}(T_{in})\right] + x_{N_2}\left[H_{m,N_2}(T_{bed}) - H_{m,N_2}(T_{in})\right]\}, \quad (3.6)$$

which we can simplify as follows:

$$\dot{Q} = \dot{n}_{inlet}\{\frac{x_{CH_4,0}-x_{CH_4}}{1+x_{CH_4}}\Delta H_r + x_{CH_4,0}\left[H_{m,CH_4}(T_{bed}) - H_{m,CH_4}(T_{in})\right] + x_{N_2}\left[H_{m,N_2}(T_{bed}) - H_{m,N_2}(T_{in})\right]\}. \quad (3.7)$$

## 3.4 Carbon flow rate

In Section 3.2 we calculated the energy required to maintain the process. In the circulating fluidized bed application, this energy would be supported by the hot carbon particles that are heated in a separate reactor, and which is a design problem of itself. Carbon can be heated by several methods (burning NG, hydrogen or carbon even). Now we have

$$energy\ required = energy\ supported = carbon\ flow\ rate \times heat\ capacity\ of\ carbon$$

$$\dot{Q} = \dot{n}_C C_{pm,C}\left(T_{C,in} - T_{bed}\right) \quad (3.8)$$

$$\dot{n}_C = \frac{\dot{Q}}{C_{pm,C}\left(T_{C,in} - T_{bed}\right)} \quad (3.9)$$

$$\dot{m}_C = \dot{n}_C M_C \quad (3.10)$$

Naturally, $T_{C,in}$ has to be higher than the bed temperature in order to maintain the process heat.

One suggested application is that sand would be used as fluidizing bed material. It would have the sufficient mass/volume ratio to provide the required heat in reasonable mass flow. Fine carbon is very light, thus large volume flows would be needed. In addition, fluidizing conditions are harder to control with dust-like materials.

# 4 KINETICS CONSTRAINT

## 4.1 Introducing the kinetic parameters

### 4.1.1 Activation energy

Activation energy describes the amount of energy required to initiate the chemical reactions. Therefore, activation energy determines the lower bound of the temperature at which the chemical reactions can start. Catalyst is often used to lower this barrier and initiate the desired reaction with lower energy (~temperature). Figure 4.1 illustrates the activation energy boundary both with and without the catalyst.

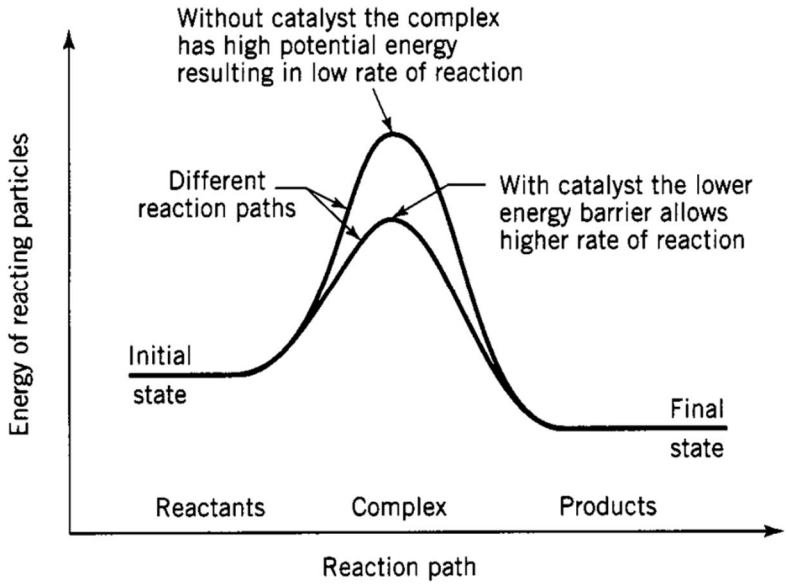


***Figure 4.1.*** *The effect of activation energy on reaction [1].*

Due to a very strong C-H bond, 440 kJ/mol, methane is one of the most stable organic molecules: thermal dissociation of methane in reasonable amounts would require temperatures in excess of 1000 °C.

### 4.1.2 Frequency factor

Frequency factor describes the upper bound for the reaction rate. It is also often called a pre-exponential factor, and sometimes steric factor. It represents a theoretical situation where all the collisions between the molecules initiate a chemical reaction. The exponential part of the Arrhenius equation (see Section 4.2) describes the number of the collisions that have enough energy to do so.

## 4.2 In general

Generally chemical reaction is of form

$$S \leftrightarrow product. \tag{4.1}$$

The rate equation or rate law is a mathematical expression used in chemical kinetics to link the rate of a reaction to the concentration of each reactant. It is of the kind

$$-r_S = k(T)[S]^n, \tag{4.2}$$

where the exponent $n$ is called the reaction order and it depends on the reaction mechanism. In this equation $k(T)$ is the reaction rate coefficient or rate constant, although it is not really a constant, because it includes all the parameters that affect reaction rate, except for concentration, which is explicitly taken into account. Of all the parameters described before, temperature is normally the most important one. Temperature dependency is often given by the Arrhenius equation:

$$k = A \exp\left(-\frac{E_a}{R_u T}\right), \tag{4.3}$$

where $A$ is the pre-exponential factor or frequency factor, and is also denoted by $k_0$ in literature. $E_a$ is the activation energy (the energy that must be overcome in order for a chemical reaction to occur), and it is given in units *kJ/mol*.

In catalytic systems the rate of reaction can be expressed in one of many equivalent ways[1], for example

based on the volume of voids in the reactor
$$-r_S = -\frac{1}{V}\cdot\frac{dn_S}{dt} = k(T)[S]^n \qquad \left[\frac{mols\ reacted}{m^3\ voids\ \cdot s}\right] \tag{4.4}$$

based on catalyst weight
$$-r_S{}' = -\frac{1}{W}\cdot\frac{dn_S}{dt} = k'(T)[S]^n \qquad \left[\frac{mols\ reacted}{kg\ cat\ \cdot s}\right] \tag{4.5}$$

based on catalyst surface
$$-r_S{}'' = -\frac{1}{S}\cdot\frac{dn_S}{dt} = k''(T)[S]^n \qquad \left[\frac{mols\ reacted}{m^2\ cat.surf.\ \cdot s}\right] \tag{4.6}$$

based on catalyst volume
$$-r_S{}''' = -\frac{1}{V_{cat}}\cdot\frac{dn_S}{dt} = k'''(T)[S]^n \qquad \left[\frac{mols\ reacted}{m^3\ solid\ \cdot s}\right] \tag{4.7}$$

based on total reactor volume
$$-r_S{}'''' = -\frac{1}{V_r}\cdot\frac{dn_S}{dt} = k''''(T)[S]^n \qquad \left[\frac{mols\ reacted}{m^3\ reactor\ \cdot s}\right] \tag{4.8}$$

based on bed volume
$$-r_S{}^* = -\frac{1}{V_{bed}}\cdot\frac{dn_S}{dt} = k^*(T)[S]^n \qquad \left[\frac{mols\ reacted}{m^3\ bed\ \cdot s}\right] \tag{4.9}$$

For porous catalyst particles rates based on unit mass and on unit volume of particles, $r_S{}'$ and $r_S{}'''$ are the useful measures.

Equations 4.2 and 4.3 are now combined, thus

$$-r_S = A \exp\left(-\frac{E_a}{R_u T}\right)[S]^n. \tag{4.10}$$

## 4.3 For TDM

The chemical reaction is

$$CH_4(g) \leftrightarrow C(s) + 2H_2(g). \tag{4.11}$$

Thus Equation 4.2 becomes

$$-r_{CH_4} = k(T)[CH_4]^n. \tag{4.12}$$

As methane is in gaseous phase, by applying the ideal gas law, following mathematical trick can be done:

$$pV = nR_u T \tag{4.13}$$

$$[CH_4] = C = \frac{n}{V} = \frac{p}{R_u T}. \tag{4.14}$$

Substituting this relation into Equation 4.12 it becomes

$$-r_{CH_4} = k(T)\left(\frac{p_{CH_4}}{R_u T}\right)^n \tag{4.15}$$

$$-r_{CH_4} = \frac{k(T)}{(R_u T)^n} {p_{CH_4}}^n \tag{4.16}$$

Thus the rate constant is merely scaled with constant values of $R_u$, $T$ and the reaction order $n$. Rewriting Equation 4.16 gives

$$-r_{CH_4} = k {p_{CH_4}}^n, \tag{4.17}$$

where $k = \frac{k(T)}{(R_u T)^n}$. It will have the corresponding unit according to the equation above. It is more practical to use partial pressures as it involves less calculation.

## 4.4 Decomposition rate

Starting from a reactor performance equation (e.g. [1]), rate can be presented as follows:

$$-r_{S,out}{}' = \frac{\dot{n}_{S,in} \cdot \chi_S}{m_{cat}}. \quad (4.18)$$

Values for the methane decomposition rate ($r$) are calculated using the following formula (e.g. [2]):

$$-r_{CH_4} = \dot{n}_{CH_4} \cdot \frac{\chi_{CH_4}}{m_{cat}}, \quad (4.19)$$

where $\dot{n}_{CH_4}$ is the molar flow rate of methane in units *mmol/min*, $\chi_{CH_4}$ is the measured methane conversion percentage and $m_{cat}$ is the weight of the catalyst. Thus $r$ has units of $mmol/g_{cat}\ min^{-1}$.

For easier calculation, Equation 4.19 can be modified as follows with the ideal gas law:

$$-r_{CH_4} = 10^{-3} \cdot \frac{p_{CH_4,inlet}\dot{V}_{CH_4}}{R_u T} \cdot \frac{\chi_{CH_4}}{m_{cat}}, \quad (4.20)$$

where $p$ is methane partial pressure at the inlet, $R_u$ the universal gas constant and $T$ the operating temperature. It is to be discussed whether the temperature should actually be the operating temperature or the standard (STP) temperature.

Initial decomposition rate $r_i$ (sometimes $r_0$) can be calculated by curve fitting (see Appendix C) from the decomposition curve, and it is used to determine the frequency factor.

## 4.5 Literature values obtained from previous experiments

Literature values for reaction kinetics estimation are collected from the literature in the Table 4.1. The values obtained by different researchers are fairly coherent thus acting as a rather reliable source material.

***Table 4.1.*** *Values for reaction kinetics, obtained from various research papers.*

| Year | Catalyst | Reaction order, $n$ | Activation energy, $E_a$[kJ/mol] | Reference |
|---|---|---|---|---|
| 2004 | AC | 0.5 | 186-198 | Kim et al. [2] |
| 2005 | AC, CB | 0.6; 0.5 | 160-201; 200-230 | Muradov et al. [4] |
| 2005 | AC | 0.5 | 117-185 | Bai et al. [5] |
| 2008 | AC, CB | ~0.5 | 141; 238 | Suelves et al. [3] |
| 2009 | AC | 0.4-0.6 | 210 | Abbas et al. [6] |
| 2010 | AC | 2 | 163 | Abbas et al. [7] |

# 5 DETERMINING BED PROPERTIES

$$bed\ volume = volumetric\ flow\ of\ methane \times residence\ time$$

$$V_{bed} = \dot{V}_{feed} \cdot \tau \tag{5.1}$$

Bed mass can be determined as follows:

$$m_{bed} = \rho_C (1 - \varepsilon) \cdot V_{bed} \tag{5.2}$$

## 5.1 Residence time for the carbon particles

Residence time for the carbon particles is denoted by $\tau_C$. It is calculated as follows:

$$\tau_C = \frac{m_{bed}}{\dot{m}_C} \tag{5.3}$$

## 5.2 Space velocity

In chemical reactor design, space velocity indicates the relation between volumetric flow and reactor volume. When a catalyst is present, the corresponding catalyst volume is often used. The notation for the space velocity is SV and it is related to the residence time in a chemical reactor, $\tau$, by the relationship

$$SV = \frac{\text{volumetric flow}}{reactor\ volume} = \frac{1}{\tau}. \tag{5.4}$$

The space velocity indicates how many reactor volumes of feed can be treated in a unit time. Usually the reference time is one hour, and the values presented hereafter refer to the volume hourly space velocity (VHSV). Furthermore, if we consider the reactor dimensions to be unchanged and the catalyst density to be constant, we can deduce that the catalyst mass increase is linearly proportional to the catalyst volume:

$$VHSV = \frac{\text{volume of gas feed / hour}}{volume\ of\ catalyst} = \frac{1}{\tau}. \tag{5.5}$$

Abbas and Daud concluded after their measurements in [17], that the initial methane decomposition rate was enhanced by the increase of the VHSV. In order to

increase the VHSV, either the gas feed rate is increased or the catalyst volume (mass) is decreased. This is obvious from Equation 5.5, and is also consistent with the results published in the literature. The rate of decomposition seemed to be more sensitive to the change in the gas feed rate than to the mass change, but only at a relatively large VHSV. It can be presumed that with different catalyst materials we might end up with different absolute values, but the trends would remain the same.

Some research papers apply space velocity in terms of the mass of the catalyst. The author would like to discuss the use of the weight-based space velocity. Especially when dealing with porous media, like the catalysts used here, it is convenient to use the mass instead of volume, as determining the density of a porous material is not very straightforward. However, the catalyst bed volume seems to affect strongly the methane decomposition reaction. Mass-based space velocity does not give the information about the bed to a reader. For example, sand used in our experiments was many times denser than the carbon black. Samples with the same weight would have the same space velocities in terms of the mass, but drastically different bed heights leading to different residence times. Thus, in the future, the characterization of the carbon catalyst should also include the density measurements, and the use of volume-based space velocity is recommended.

# 6 EXPERIMENTS ON CATALYSTS

## 6.1 Materials

Methane (99.995%) and nitrogen from Linde Group were used without further purification.

The quartz tubes, (I.D 26mm) was supplied by Quartz Inc. (the U.S). The stainless steel reactor vessel was constructed of AISI 309 (X15CrNiS 20/12).

Commercial carbon black, BP2000 was supplied by Cabot Corporation (the U.S.). The bulk volume of CB was sieved to desired fractions. The biomass-based activated carbon was made in our laboratory, and the process is described in Section 6.3.

## 6.2 Experimental set-up

The experimental apparatus used is based on the designs found in the research reports, and also on the experiences with the first version during the FP I. A new reactor was built, and different oven type was used to support the heat. The reactor lid was at the cold end, thus maintaining its tightness. A quartz cylinder, with kaowool grates, was used to contain the catalyst sample, both to avoid the stainless steel from affecting the reactor and making it possible to weigh the sample before and after the run. The cylinder was tightened into the outer vessel by wrapping a ceramic band around it and lowering it into the holder at the bottom of the stainless steel reactor.

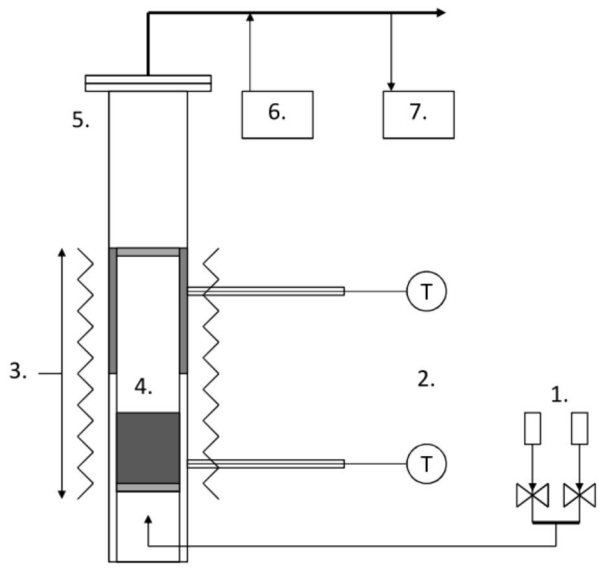


| # | **Component** |
|---|---|
| 1. | Bronkhorst mass flow controllers |
| 2. | K-type thermoelements |
| 3. | Heated reactor length, 590 mm |
| 4. | quartz cylinder |
| 5. | sealed lid |
| 6. | diluting gas for FTIR |
| 7. | sample for FTIR |

***Figure 6.1.*** *Schematic diagram of the decomposition reactor.*

The run length was set to approximately 150 minutes, with 100% methane in every run. The gas samples were continuously analyzed by a Fourier transform infrared (FTIR) gas analyzer. The analyzer is unable to directly measure diatomic gases – hydrogen, for example - thus the amount of hydrogen formed has to be calculated from the difference between the methane in the inlet and outlet flows.

## 6.3 Char production

Locally available and cheap, domestic birch (*Betula sp.*) was selected to be the raw material for the char production. The fire wood sized wood was chipped to thin sticks and heated in the oven at 500 °C for 1.5 hours in an inert atmosphere. There was a clear pulse of volatile compounds rapidly releasing from the wood at approximately 450 °C, for 10-15 minutes. after the run, the charred sample was weighed yield being approximately 20% of the original weight.

The charred wood was crushed and sieved to desired sizes. During the first runs the char still seemed to release some volatile compounds. Thus the crushed and sieved samples were further heated up to 825 °C for approximately an hour to completely remove the unwanted components. The weight loss was between 5-10% compared to the wood pyrolyzed at 500 °C. This leads the author to think the actual operating window temperaturewise is quite narrow when dealing with birch. Relatively high temperatures are required to remove all the volatiles, but only little higher temperatures already cause the ash component to go through a deformation indicating there would not be too much alternatives in the design parameters.

# 7 RESULTS AND DISCUSSION

Different catalyst materials tested in 2012 were quartz sand, pure quartz, biomass-based active carbon and commercial carbon black. Of the aforementioned, active carbon and carbon black went through more thorough tests.

Sand was taken into account, because one potential TDM-process could apply sand as a heat transfer material. In a bubbling or circulating fluidized bed, sand is the common material because of its adequate heat capacity and fluidization properties. In addition, some research conducted with metal-based catalysts in TDM applied quartz as a support material for the metal particles has yielded positive results.

To determine whether sand or pure quartz (Nilsiä) have either positive or negative effect on the reaction, we carried out runs varying the reaction temperature, catalyst mass and particle size. After only few runs it became evident that in our conditions, neither material had any kind of effect to the decomposition reaction. As a side note, in the reaction temperature 925 °C the Nilsiä quartz bed show symptoms of sintering thus making it even less feasible.

Before the actual runs, catalyst was treated with a constant flow of nitrogen for approximately two hours to remove the possible remaining moisture and surface pertained oxygen. It is to be noted, that according to literature, the oxygen adsorbed in the pores is very difficult to remove by mere flushing.

During the runs, only trace amounts of other compounds were detected.

## 7.1 Runs with biomass based char

The goal of the experiments was to determine the catalytic potential of a cheap, domestic biomass based char towards TDM. Runs conducted in temperatures under 900 °C showed modest catalytic activity (initial conversion percentage ~10%) but in 15-30 minutes rapidly declined to practically zero. To achieve higher conversions, reaction temperature was raised to 925 °C. Oddly, conversion was lower (~3%) than in the runs in lower temperatures. Due to the constant value it could solely be attributed to the homogenous decomposition taking place in elevated temperatures.

As the run was over and the measuring cylinder removed from the reactor, we observed the bed had gone through a deformation. The catalyst particles had taken a shape of a cylinder, i.e. ‘glued’ to each other. Only when the bed was poured out of the vessel, particles separated. This could indicate, that the ash component cannot withstand temperatures above 900 °C without a change in its structure, i.e. at least partial melting. This indication was strengthened, when we had the particle surface areas measured. The original surface area before the runs was 352 $m^2/g$, whereas after the run it was only 1,1

$m^2/g$. The pores in the particles seem to go through a heavy deformation thus blocking the favorable and active sites for the gas molecules to enter. Based on our observations, with the current production method, the biomass based active carbon is not suitable towards thermocatalytic decomposition of methane. Different chemical treatments to remove or alter the ash component might offer a solution.

## 7.2 Runs with the commercial carbon black

Again, high surface area carbon black BP 2000 was selected to be the catalyst for our tests. Although the actual particle size is in nanometer scale, the particles have agglomerated, forming larger carbon spheres. Particles were mechanically sieved to desired fractions. All the particle sizes used were in between 100-600 μm. To our best understanding, the effect of the particle size is weak, at least in this relatively narrow range. Kim and Abbas have also obtained similar results. Diffusional limitation studies have been done by Abbas and Daud [7], and they have concluded that a mass transfer effect exists.

If the application used will be a fluidized bed reactor, it means that there is also a lower boundary for the particle size due to fluidization requirements (See more, Geldart; Kunii & Levenspiel).

### 7.2.1 Effect of temperature

As the temperature is a critical parameter in the decomposition reaction, its effect was evaluated with two different sets of runs, when the other process parameters remained the same. The parameters used in the first set of runs are listed in Table 7.1. All the volumetric values presented in the text are given in STP conditions.

***Table 7.1.*** *Parameters used in runs to determine the effect of temperature (set 1).*

| | | | |
|---|---|---|---|
| pressure | p | 1 | atm (amb.) |
| methane flow rate | $\dot{V}_{CH4}$ | 0.050 | l/min |
| methane mole fraction | $x_{CH4}$ | 100 | % |
| catalyst mass | $m_{cat}$ | 5 | g |
| space velocity | | 144 | 1/h |

In the first set, four different temperatures were used. Figure 7.1illustrates the runs in terms of the % of methane converted.

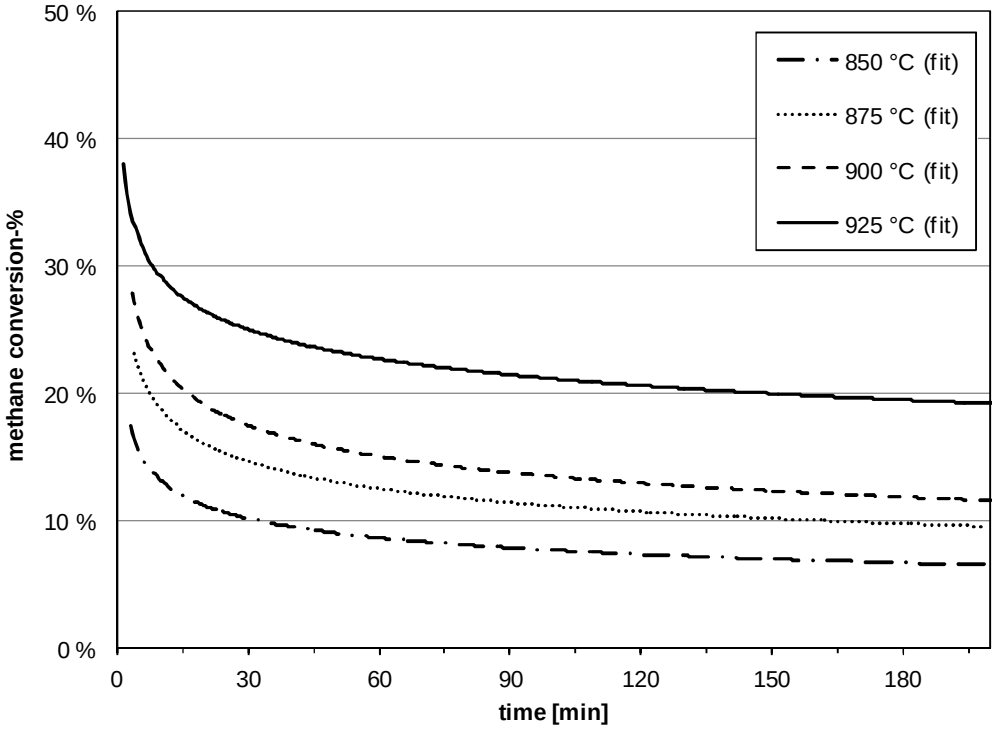


**Figure 7.1** *The effect of temperature on the % of methane converted (set 1: 50 $ml_{CH4}$/min; 5g).*

Due to the method the runs were conducted, the stabilization time was 5-15 minutes. The initial steep part of the graph had to be fitted based on the actual measured and calculated values. The same method was used, and similar behaviour can be observed in all the runs. The gap between the runs conducted in 900 and 925 °C seems to be somewhat larger than in between the others. Partial reason can be that homogenous decomposition, i.e. methane cracking only due to the high temperature, starts to contribute.

The accumulation of carbon in the runs was also measured. The Figure 7.2 illustrates the runs in terms of the amount of carbon generated per the mass of catalyst.

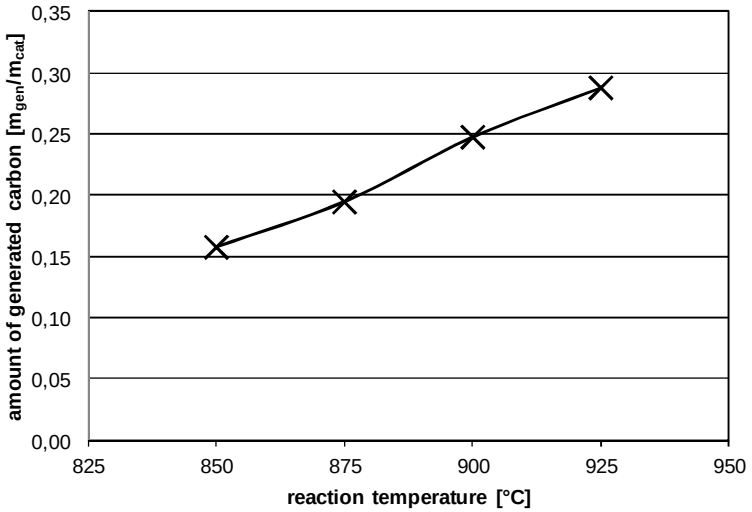


***Figure 7.2.*** *The amount of generated carbon per the amount of catalyst as a function of the reaction temperature (set 1: 50 $ml_{CH4}$/min; 5g).*

The amount of generated carbon seems to grow somewhat linearly. The generation of carbon would have continued until the reaction rate had dropped to negligible values. From available literature, for BP2000 it can take several hours to become completely deactivated. That is to say, the amount of generated carbon really is significant. In two hours, and with already relatively low conversions, it's between 20 and 30% of the original catalyst mass. Considering larger scale apparatus, this would most likely limit the use of a fixed bed reactor. Furthermore, if the extra bed material is meant to be extracted, it would also limit the use of a bubbling fluidized bed, leaving us with a circulating fluidized reactor, or with a completely new approach. The reason to consider some new approaches is that circulating fluidization would require high gas velocities. That in turn would mean higher space velocities, which is inversely correlated to the reaction conversion rate, as can be seen in Section7.2.2

The parameters used in the second set of runs are listed in Table 7.2. Now, the amount of catalyst is doubled, and temperatures 875, 900 and 925 °C are used. During the last two runs the FTIR exiting gas was also sampled, and measured in a gas gromatographic analyzer (GC) to directly measure the amount of hydrogen gas. The results confirmed our indirect calculations fairly well, and proved the superiority of the possibility to conduct continuous measurements of the gas concentrations over the sampling one.

***Table 7.2.*** *Parameters used in runs to determine the effect of temperature (set 2).*

| | | | |
|---|---|---|---|
| pressure | p | 1 | atm (amb.) |
| methane flow rate | $\dot{V}_{CH4}$ | 0.050 | l/min |
| methane mole fraction | $x_{CH4}$ | 100 | % |
| catalyst mass | $m_{cat}$ | 10 | g |
| VHSV | | 72 | 1/h |

Figure 7.3 illustrates the second set of runs in terms of the % of methane converted.

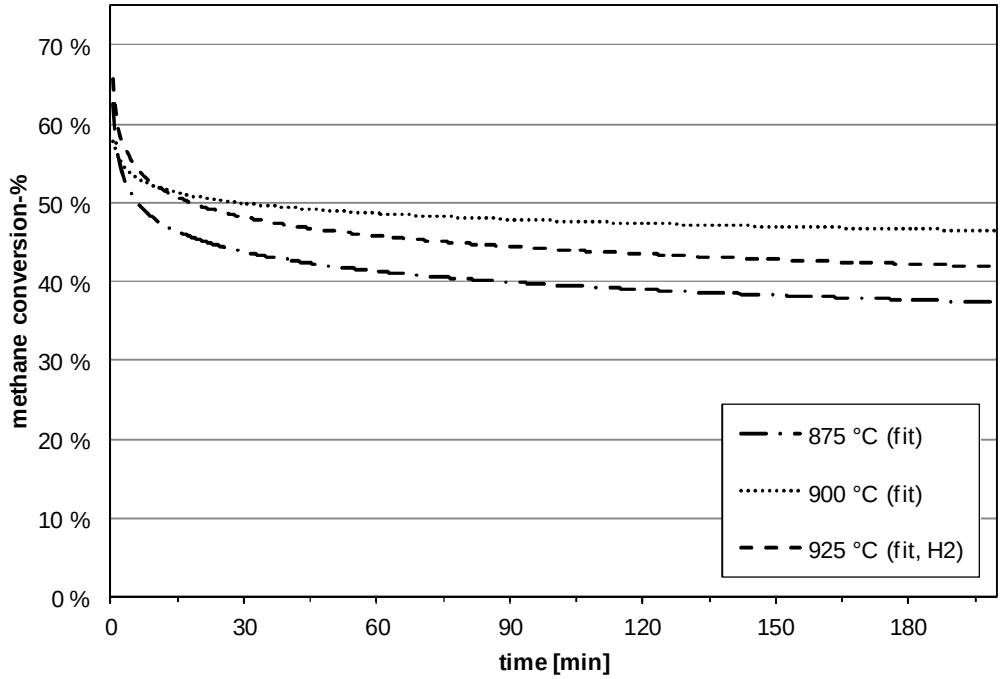


***Figure 7.3.*** *The effect of temperature on the % of methane converted (set 2: 50 $ml_{CH4}$/min; 10g).*

It is to be noticed, that the conversion is remarkably higher than with the lower amount of catalyst. Also, the 'tail' that can be described as a quasi-steady state of conversion is more horizontal than in the runs described previously. As the high values of conversion are reached only during the first minutes of the run, the area of interest should maybe more guided towards the relatively steady phase, where the yields of hydrogen and carbon can more precisely be estimated.

The conversion graph for 925 °C is fitted based on the hydrogen values, and is actually slightly lower than the 900 °C graph. This can be attributed to the different method of making the conversion calculations. As there was problems with the catalyst bed in the last run, carbon accumulation values are available only for the first two runs, and presented in the Table 7.3.

***Table 7.3.*** *The amount of generated carbon per the amount of catalyst as a function of the reaction temperature (set 2: 50 $ml_{CH4}$/min; 10g).*

| temperature | amount of generated carbon per mass of catalyst |
|---|---|
| °C | $g/g_{cat}$ |
| 875 | 0,141 |
| 900 | 0,184 |

The values seem to be lower than in the runs conducted with 5 grams of catalyst (see Figure 7.2). This leads the author to think that increasing the bed volume also has some unaccounted effect on the reaction, outside of decreasing the space velocity. Similar pattern can be found in the runs, where the space velocity was held constant, but the amount of catalyst and the gas flow were varied (see Section 7.2.2).

### 7.2.2 Effect of the space velocity

After the runs conducted during the FP I, it became evident, that the lower the space velocity, the higher the methane conversion percentage is. It was deduced, that the reactions taking place in the catalyst bed are not immediate, and the residence time of methane has to be rather seconds than fractions of it. During the runs, the advantages of presenting the space velocity in terms of volume became clear. This was discussed in Section 5.2. The parameters used in the set 3 runs are listed in Table 7.4:

***Table 7.4.*** *Parameters used in runs to determine the effect of space velocity (set 3)*

| | | | |
|---|---|---|---|
| temperature | T | 900 | °C |
| pressure | p | 1 | atm (amb.) |
| methane flow rate | $\dot{V}_{CH4}$ | 0.050 | l/min |
| methane mole fraction | $x_{CH4}$ | 100 | % |

| | **run 1** | **run 2** | **run 3** |
|---|---|---|---|
| catalyst mass | 5 g | 7.5 g | 10 g |
| VHSV | 144 1/h | 96 1/h | 72 1/h |

Figure 7.4 illustrates the runs in terms of the % of methane converted.

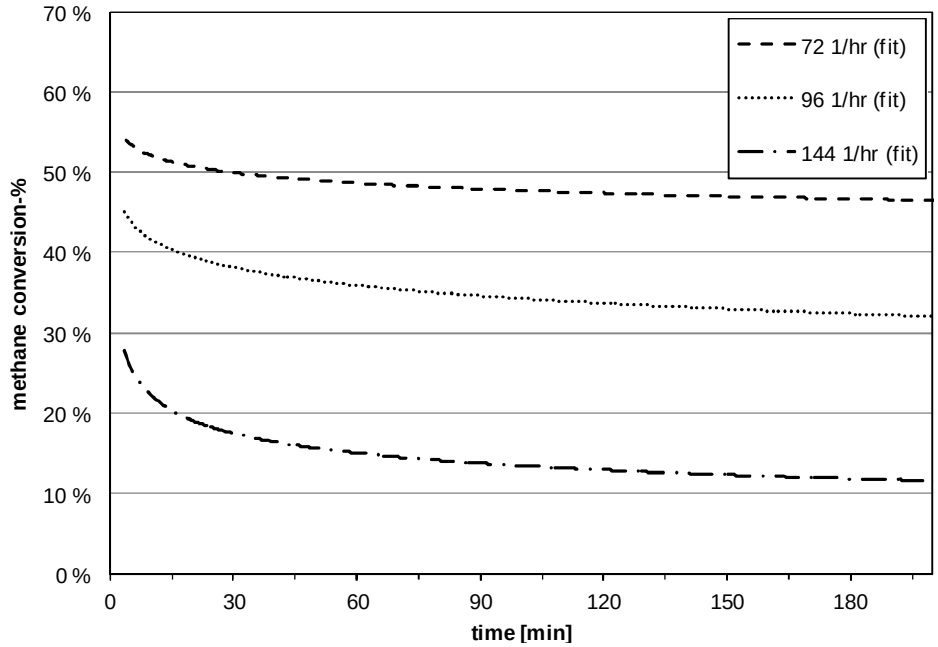


***Figure 7.4.*** *The effect of space velocity on the % of methane converted (set 3: 50 $ml_{CH4}$/min; 5g, 7.5g, 10g; 900 °C).*

As can be seen from the Figure 7.4, the space velocity has a drastic effect on the conversion. Also the steepness of the initial curve, and the quasi-steady state are affected. Notable here is that with the gas flow rate used, we operated in a fixed bed mode. The space velocities used here are most likely out of question in a large scale application.

To see how the conversion rate would behave, when the space velocity was held constant but the amount of catalyst and the flow rate of methane were changed, few test runs were conducted. The parameters used in the set 4 runs are listed in Table 7.5:

***Table 7.5.*** *Parameters used in runs to determine the effect of space velocity (set 4)*

| | | | |
|---|---|---|---|
| temperature | T | 900 | °C |
| pressure | p | 1 | atm (amb.) |
| methane mole fraction | $x_{CH4}$ | 100 | % |
| VHSV | | 144 | 1/h |

| | **run 1** | **run 2** | **run 3** |
|---|---|---|---|
| catalyst mass | 5 g | 10 g | 15 g |
| methane flow rate | 50 ml/min | 100 ml/min | 150 ml/min |

Figure 7.5 illustrates the runs in terms of the % of methane converted.

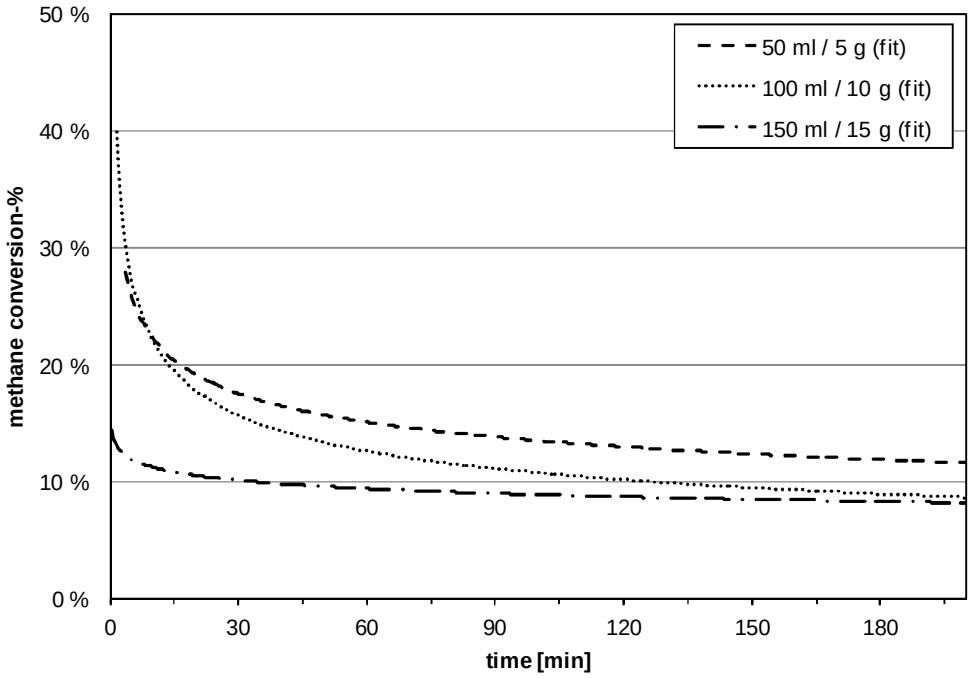


***Figure 7.5.*** *The effect of space velocity on the % of methane converted (set 4: 144 1/h; 900 °C).*

Initial differences are larger, than one would assume, but as the runs continue, the graphs approach each other. The notions here are, that the lowest yield obtained with the highest methane flow rate could partially be due to the possible change in the bed state. With the mentioned flow rate, the minimum fluidization velocity might have been reached. The bubbles formed can block the gas of entering the catalyst pores thus lowering the conversion.

Here we were able to determine the mass change of the catalyst. The Figure 7.6 illustrates the runs in terms of the amount of carbon generated per the mass of catalyst.

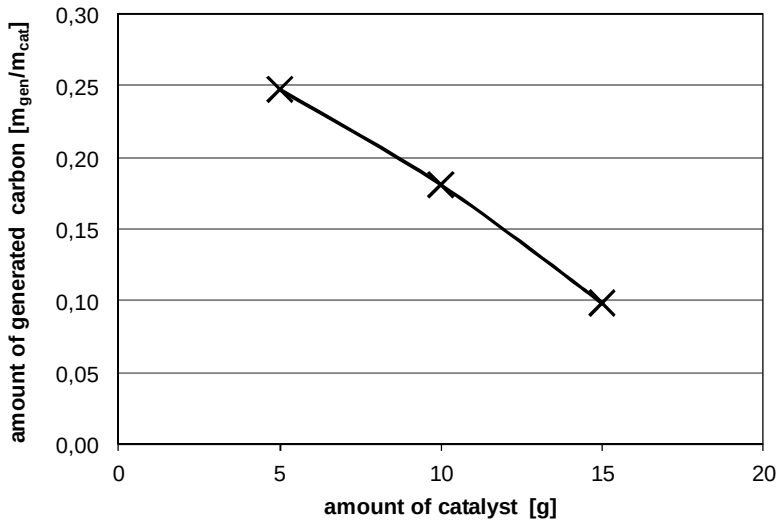


***Figure 7.6.*** *The amount of generated carbon per the amount of catalyst as a function of the reaction temperature (set 4: 144 1/h; 900 °C).*

As mentioned earlier, in our experiments it seemed that the larger the volume of the catalyst bed, the less generated carbon per mass unit. This behaviour might be due to some diffusional resistance in a larger catalyst bed.

### 7.2.3 Decomposition rates

Decomposition rates for the methane decomposition reaction were calculated with the method described in Section 4.4. As can be seen from the Figure 7.7, rather modest reaction rate values were obtained. In the literature, as high as unity has been reported for the initial decomposition rate value. It is to be noted, however, that the high initial values have been present with the use of metal catalysts. Metal catalysts in general offer a rapid initial decomposition rate with quick decline, whereas carbon based catalysts show more steady behaviour.

a)

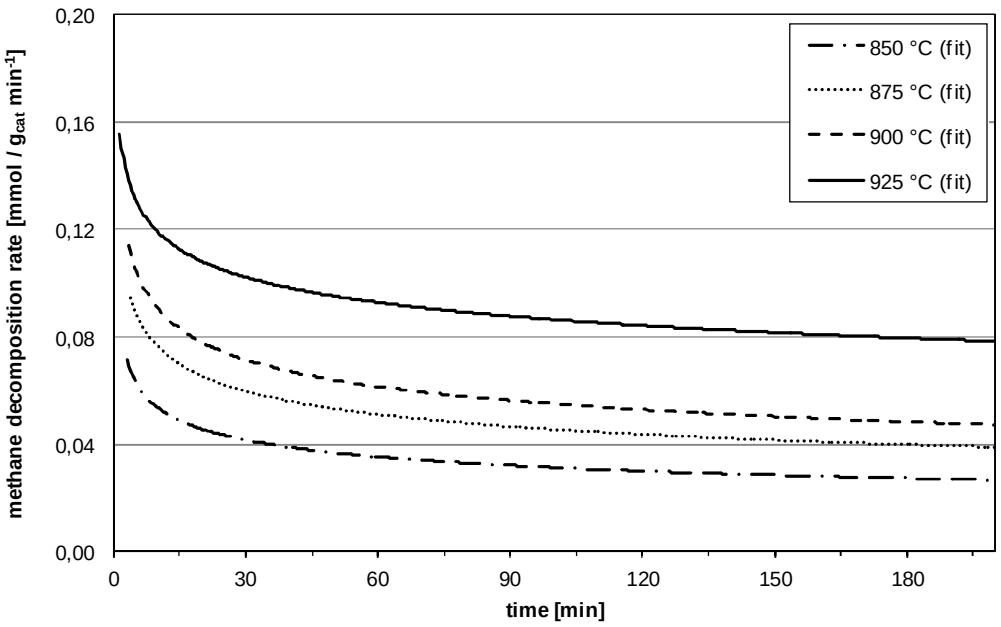


b)

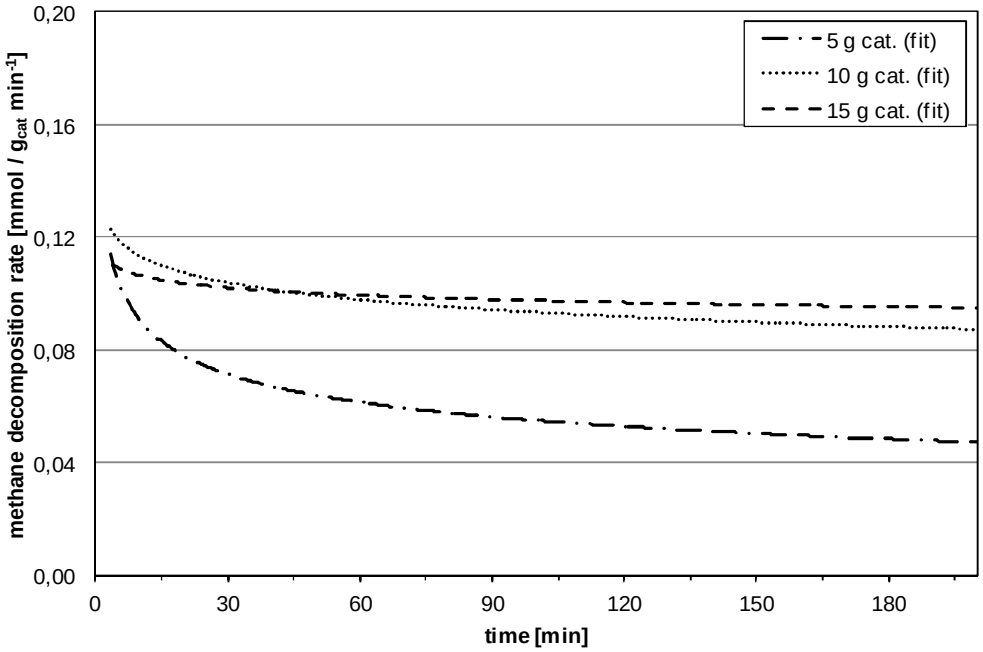


***Figure 7.7.*** *Methane decomposition rate as a function of a) temperature (set 1) and b) space velocity (set 3).*

### 7.2.4 Nature of the carbon generated

Prior to the runs, the assumption was that the carbon formed by methane decomposition would accumulate on the surface of the catalyst particles. That is also where the most reactions occurred. A strong indication of this was, when we had the the surface areas measured for one catalyst both before and after a run. The Brunauer-Emmett-Teller (BET) surface area measurement confirmed that the carbon black catalyst had lost almost 80% of its initial surface area. The details are shown in Table 7.6.

***Table 7.6.*** *Results of BET-surface area measurements*

| | | | |
|---|---|---|---|
| temperature | T | 925 | °C |
| pressure | p | 1 | atm (amb.) |
| run time | t | 150 | min |

| BET-surface areas | | |
|---|---|---|
| initial | 1483 | $m^2/g$ |
| final | 333.4 | $m^2/g$ |
| change | 77.5% | |

In the BET-measurement results, there was a clear spike at 0.5-0.7 nm pores in the fresh catalyst. This spike had reduced 79% after the run, indicating this might be the desirable pore size for the decomposition reaction to occur. It should be noted, however, not to draw too strong conclusions based on a single result. Further ones should be obtained before confirming this.

During the runs, we observed also flaky opaque structure forming on the inner surface of the quartz tube. Further analysis showed the layer is pure carbon, but unfortunately we were not able to determine the crystallic structure due to a measuring equipment breakdown. Based on the previous research in the area, the structure is likely graphitic. Magnified pictures of the structure can be found in the Appendix D.


***Figure 7.8.*** *Material sample obtained form the quartz tube surface after a run.*

Also, during one of the runs, we observed clear carbon filamentous structures that had grown on the outer surface of the quartz tube. This was a one-time phenomenon only, thus the suitable conditions for the growth remain undetermined.

As a conclusion we can make a hypothesis, that by altering the reaction conditions we are able to change the nature of the generated carbon. This might offer us a marketable byproduct contributing to the overall process economy. Similar observations have been made by other authors as well.

## 7.3 Short summary of the funding period I results

During FP I, a literature and patent review was made. Based on the reviews, a short set of experimental runs was conducted. The results of these measurements are briefly summarized here. Also, as the understanding of the topic grew, novel ideas for the future focus areas were proposed. The proceedings of the first year are crystallized in a Master's Thesis 'Thermocatalytic Decomposition of Methane' by the undersigned author. As usual, when the knowledge deepens, it is easier to notice what could have been done better. We've tried to take the lessons from the past into account for this year's measurements.

By comparing the results herein, and the ones obtained during FP I leads the author to think that the diluting nitrogen gas has a different effect on the space velocity than previously thought. Otherwise, there is no proper explanation to how the high conversions could be obtained with such high space velocities. Thus, the conversions obtained during the first funding period are results of lower space velocities than mentioned in the publication. Also the unaccounted effect of a larger bed volume, as discussed earlier, might have contributed. The gap present in the figures was found to origin from an issue with the analysis software and it has been fixed. The previous results are summarized in the following figures:

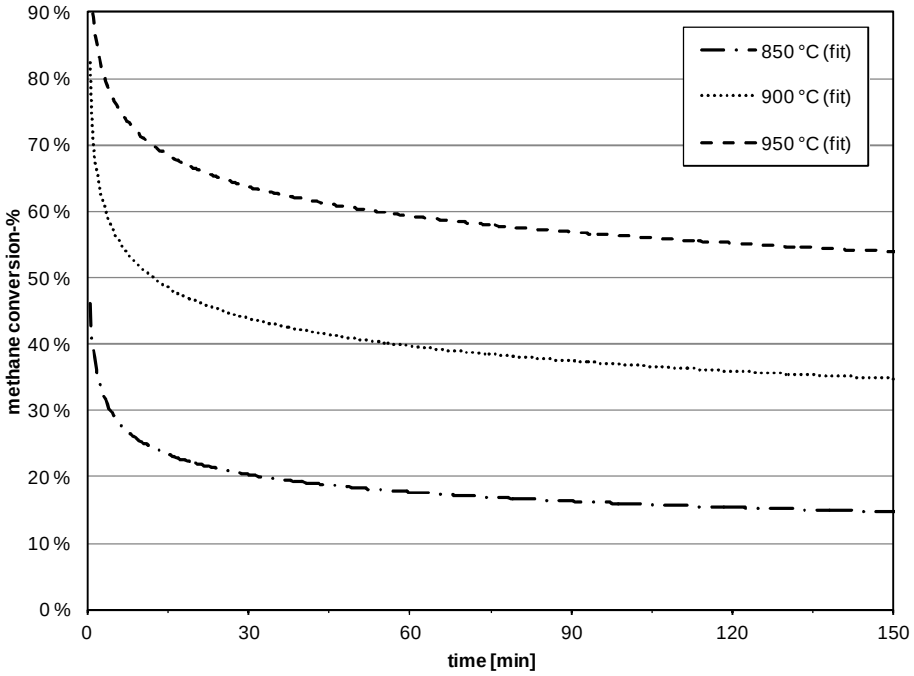


***Figure 7.9.*** *The effect of temperature on the % of methane converted (FP I: 206 $ml_{CH4}$/min; 50g).*

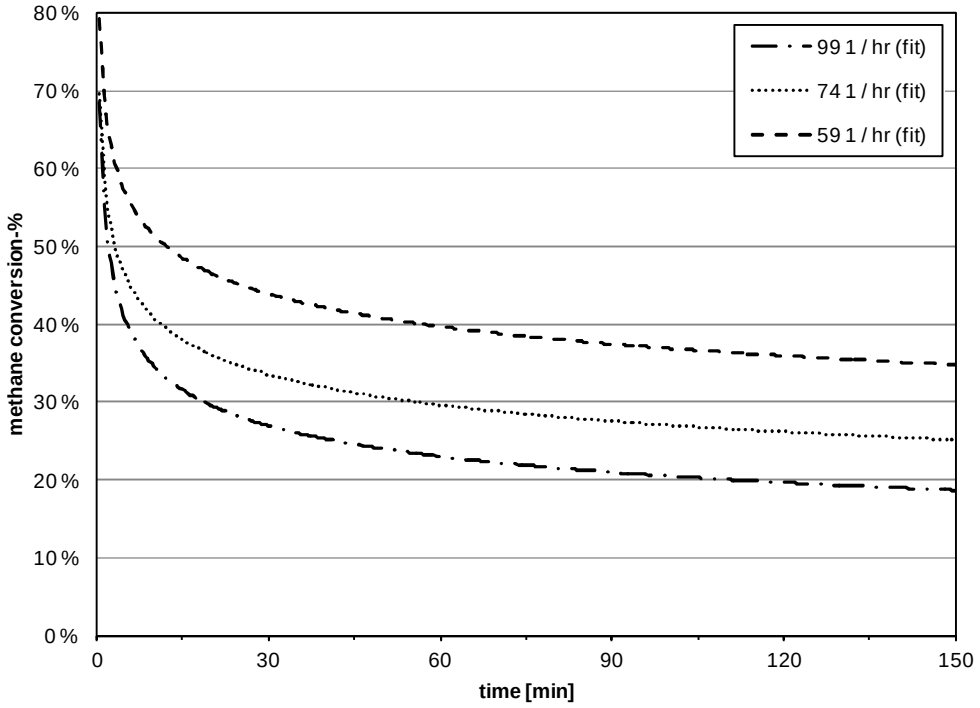


***Figure 7.10.*** *The effect of space velocity on the % of methane converted (FP I: 206 $ml_{CH4}$/min; 30g, 40g, 50g; 900 °C).*

By comparing the results obtained during FP I and FP II, we notice the similarity in the patterns. This can be taken as a confirmation of the reaction taking place rather predictably, and also of the significance of certain process parameters.

## 7.4 Future suggestions

Based on the tests and experiences during the project, we have come up with some new suggestions for the future research.

The temperatures and space velocity values required to reach even moderate reaction conversions were found. However, in a large-scale use they might cause not only designing problems, but also be economically challenging.

As can be found in the literature, metal catalysts used to enhance the decomposition reaction have given good results. With metals, the operating conditions are often more trivial thus lowering the costs. Issues in their use were discussed in the Master's Thesis 'Thermocatalytic decomposition of methane'. Our idea is that a commercially available metal catalyst combined with our current decomposition method could already offer a simple solution in the beginning phase, when trying to tackle $CO_2$-emissions in natural gas combustion. The two figures are meant to illustrate how close we are the equilibrium state of the methane decomposition reaction.

a)

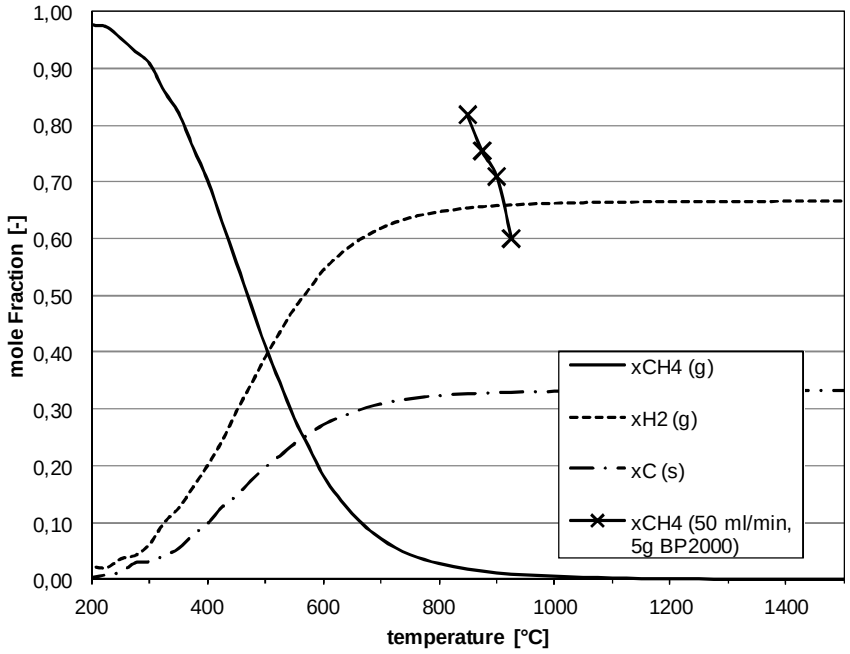


b)

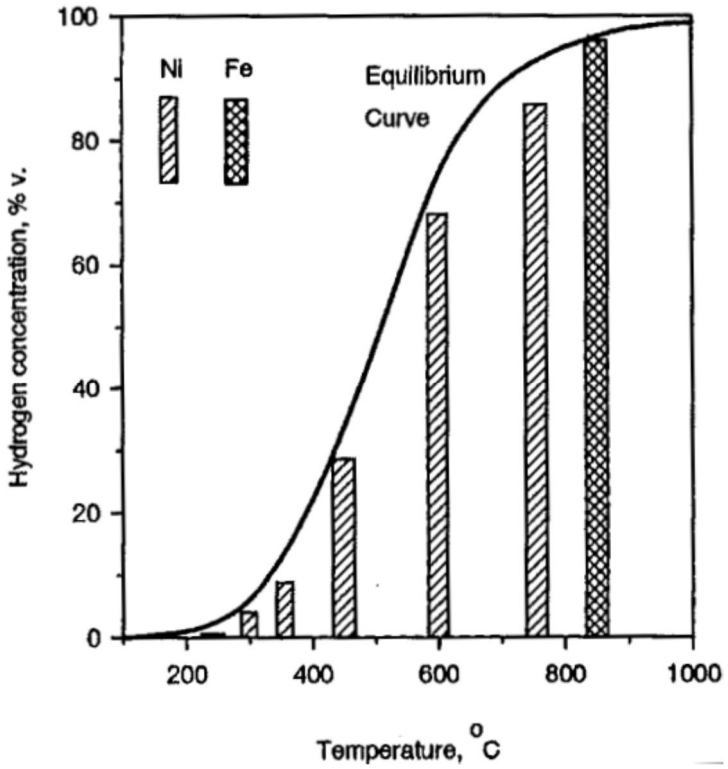


***Figure 7.11.*** *Comparison of equilibrium and measured values with a) carbon catalysts (set 1) , b) metal catalysts (printed without permission from [9])*

It can be seen from the figures that with carbon-based catalyst, the equilibrium concentration differs significantly from the measured values. By optimizing the process conditions, it could be possible to approach the theoretical graph, but only to some extent. Figure 7.11b is a result of Muradov's research [9], and shows the results they obtained through the measurements with Nickel- and Iron-based catalysts. It shows, that at seemingly lower temperatures, conversations only limited by the equilibrium were

achieved. Thus the author suggests taking selected metal-based catalysts into consideration in the future research.

Catalyst regeneration, for both metallic and carbon-based ones, could be a future area to examine. If the metals are taken into research, comparison between the regeneration behaviour between the different types could be made, and also in general.

For some future applications, it would be in the interest to research the combination of higher temperatures (in excess of 1000 °C) and carbon-based catalyst.

# 8 CONCLUSIONS

During the Cleen CCSP-program funding period II, the methane decomposition reaction to produce hydrogen and solid carbon was evaluated. As the reaction is favored by the presence of a catalyst, different catalysts were tested to gain more information of the catalyst requirements.

One potential heat carrier material, quartz sand was found to have no effect on the reaction. The domestic biomass based activated carbon showed little activity in the lower temperatures, but quickly deactivated. In the elevated temperature the carbon lost its surface area completely possibly due to the ash component melting. Tests with the commercial carbon black, BP2000 were continued and compared to the ones conducted during the FP I. With the commercial carbon black, conversion percentages around 50 % are achievable.

Essential parameters, supported both by the theory and experiments, are the reaction temperature, space velocity and catalyst surface properties.

With difficulties obtaining high conversion at moderate temperatures, the use of metal catalysts in the thermocatalytic decomposition of methane could be evaluated in the future. Novel approach could be a LUVO-type heat exchanger where the decomposition would take place.

We learned that it is difficult to design an experimental apparatus that has a large range of variables so that the reaction conditions would still be the same. It would be in the author’s interest to see the results of an experiment one magnitude larger in terms of catalyst amount and gas flow rate.

# ACKNOWLEDGEMENTS

This work was a part of the Cleen CCSP research program, and supported by Gasum Oy, Fortum Power & Heat and Helen. This work was also financially supported by the Fortum Foundation, to whom the author would like to express gratitude.

# REFERENCES


1. **Levenspiel, Octave.** *Chemical reaction engineering, 3rd ed.* : John Wiley & Sons, 1999. p. 668.

2. **Kim, Myung Hwan et al.** *Hydrogen production by catalytic decomposition of methane over activated carbons: Kinetic study.* International Journal of Hydrogen energy 29(2004), Elsevier Ltd, pp. 187-293.

3. **Muradov, Nazim;Smith, Franklyn and T-Raissi, Ali.** *Catalytic activity of carbons for methane decomposition reaction.* Catalysis Today 102-103(2005), Elsevier B.V. pp. 225-233.

4. **Chen, Haokan et al.** *Catalytic decomposition of methane over activated carbon.* J. Anal. Appl. Pyrolysis 73(2005), Elsevier B.V. pp. 335-341.

5. **Suelves, I. et al.** *Kinetic study of the thermal decomposition of methane using carbonaceous catalysts.* Chemical engineering journal 138(2008), Elsevier B.V. pp. 301-306.

6. **Abbas, Hazzim F. and Wan Daud, W.M.A.** *Thermocatalytic decomposition of methane using palm shell based activated carbon: Kinetic and deactivation studies.* Fuel processing technology 90(2009), Elsevier B.V. pp. 1167-1174.

7. **Abbas, Hazzim F. and Wan Daud, W.M.A.** *Hydrogen production by thermo-catalytic decomposition of methane using a fixed bed activated carbon in a pilot scale unit: Apparent kinetic, deactivation and diffusional limitation studies.* International Journal of Hydrogen energy 35(2010), Elsevier Ltd, pp. 12268-12276.

8. **Abbas, Hazzim F. and Wan Daud, W.M.A.** *Infuence of reactor material and activated carbon on thermocatalytic decomposition of methane for hydrogen production.* Applied Catalysis A: General 388(2010), Elsevier B.V. pp. 232-239.

9. **Muradov, Nazim Z.** *CO2-free production of hydrogen by catalytic pyrolysis of hydrocarbon fuel.* Energy & Fuels 12(1998), American Chemical Society. pp. 41-48.

# APPENDIX

## APPENDIX A – Tabulated values for equilibrium constant of methane decomposition reaction

| Equilibrium constant towards methane decomposition reaction, lg ($K_{p,decomp.}$) | | | |
|---|---|---|---|
| **T [K]** | **T [°C]** | **NIST-JANAF** | **P&P** |
| 100 | -173 | -33.615 | - |
| 200 | -73 | -15.19 | - |
| 250 | -23 | -11.395 | - |
| 298.15 | 25 | -8.894 | -8.892 |
| 300 | 26 | -8.813 | -8.811 |
| 350 | 76 | -6.932 | -6.956 |
| 400 | 126 | -5.492 | -5.489 |
| 450 | 176 | -4.35 | -4.335 |
| 500 | 226 | -3.42 | -3.418 |
| 550 | 276 | | -2.600 |
| 600 | 326 | -1.993 | -1.989 |
| 650 | 376 | | -1.426 |
| 700 | 426 | -0.943 | -0.940 |
| 750 | 476 | | -0.511 |
| 800 | 526 | -0.138 | -0.134 |
| 850 | 576 | | 0.203 |
| 900 | 626 | 0.500 | 0.504 |
| 950 | 676 | | 0.776 |
| 1000 | 726 | 1.018 | 1.022 |
| 1050 | 776 | | 1.246 |
| 1100 | 826 | 1.447 | 1.451 |
| 1150 | 876 | | 1.639 |
| 1200 | 926 | 1.807 | 1.812 |
| 1250 | 976 | | 1.972 |
| 1300 | 1026 | 2.115 | 2.119 |
| 1350 | 1076 | | 2.256 |
| 1400 | 1126 | 2.379 | 2.383 |
| 1450 | 1176 | | 2.502 |
| 1500 | 1226 | 2.609 | 2.613 |
| 1550 | 1276 | | 2.717 |
| 1600 | 1326 | 2.81 | 2.815 |
| 1650 | 1376 | | 2.907 |
| 1700 | 1426 | 2.989 | 2.993 |
| 1750 | 1476 | | 3.074 |
| 1800 | 1526 | 3.147 | 3.151 |
| 1850 | 1576 | | 3.224 |
| 1900 | 1626 | 3.289 | 3.293 |
| 1950 | 1676 | | 3.358 |
| 2000 | 1726 | 3.416 | 3.420 |

**APPENDIX B – Homogenous methane decomposition: Conversion percentage as functions of temperature and pressure**

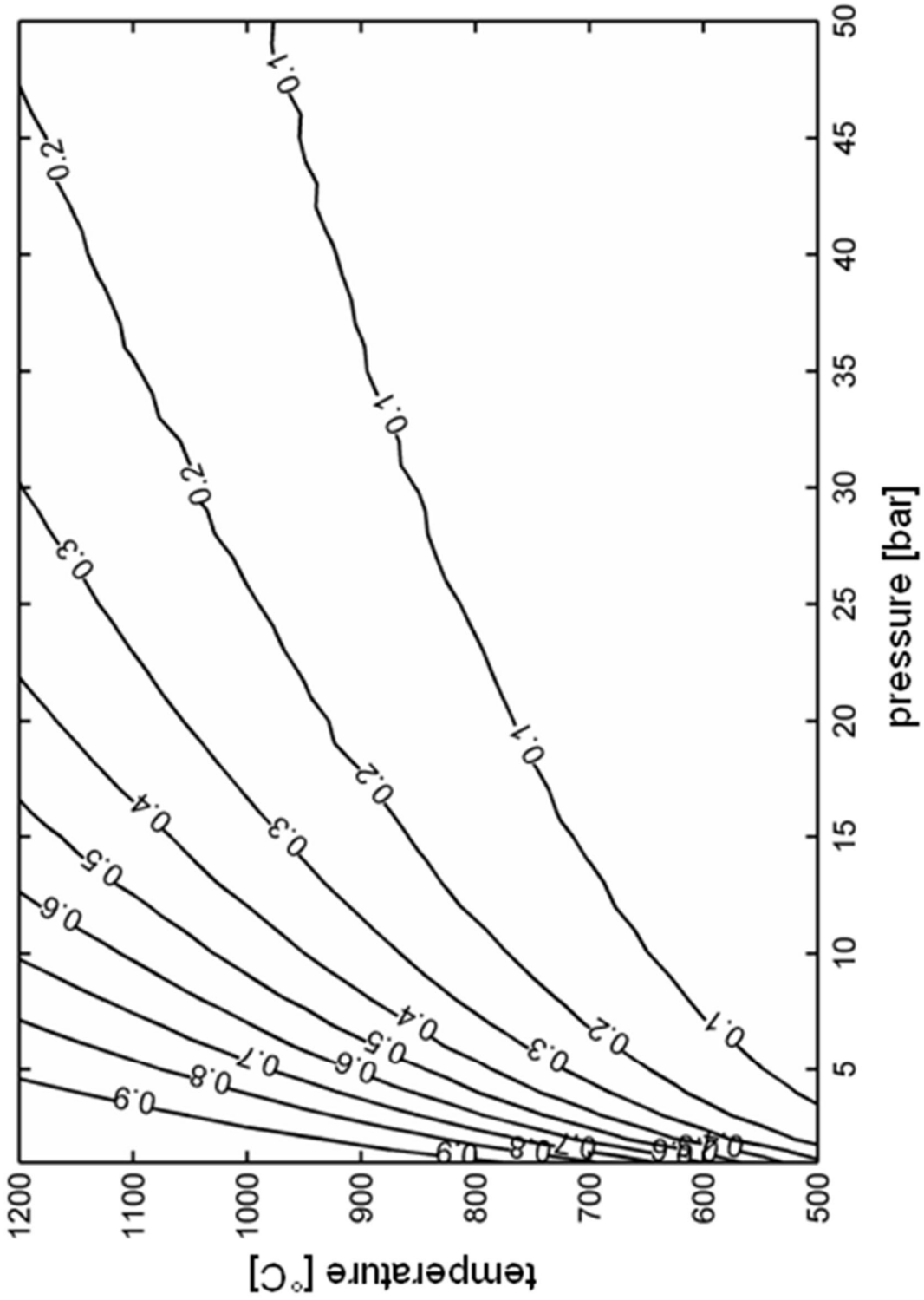

## APPENDIX C - Tabulated values for enthalpies and specific heat capacities for selected substances

| Formation enthalpy, $\Delta H_f$ [kJ/mol] | | | | | |
|---|---|---|---|---|---|
| $CH_4(g)$ | | | | | |
| **T[K]** | **T[°C]** | **Muradov** | **NIST-JANAF** | **Barin, I.** | **AsTher** |
| 298.15 | 25 | 75.6 | 74.873 | 74.873 | 74.872 |
| 300 | 27 | | 74.929 | 74.93 | 74.931 |
| 350 | 77 | | 76.461 | | 76.484 |
| 400 | 127 | | 77.969 | 77.986 | 77.969 |
| 450 | 177 | | 79.422 | | 79.383 |
| 500 | 227 | | 80.802 | 80.824 | 80.726 |
| 550 | 277 | | | | 81.995 |
| 600 | 327 | | 83.308 | 83.331 | 83.19 |
| 650 | 377 | | | | 84.312 |
| 700 | 427 | | 85.452 | 85.48 | 85.36 |
| 750 | 477 | | | | 86.333 |
| 800 | 527 | | 87.238 | 87.27 | 87.232 |
| 850 | 577 | | | | 88.058 |
| 900 | 627 | | 88.692 | 88.722 | 88.81 |
| 950 | 677 | | | | 89.488 |
| 1000 | 727 | | 89.849 | 89.876 | 90.092 |
| 1050 | 777 | | | | 90.623 |
| 1100 | 827 | | 90.75 | 90.773 | 91.081 |
| 1123 | 850 | 89.75 | | | 91.281 |
| 1150 | 877 | | | | 91.497 |
| 1173 | 900 | 89.989 | | | 91.67 |
| 1200 | 927 | | 91.437 | 91.454 | 91.855 |
| 1250 | 977 | | | | 92.157 |
| 1300 | 1027 | | 91.945 | 91.954 | 92.407 |
| 1350 | 1077 | | | | 92.608 |
| 1400 | 1127 | | 92.308 | 92.304 | 92.765 |
| 1450 | 1177 | | | | 92.882 |
| 1500 | 1227 | | 92.553 | 92.531 | 92.962 |

Fit based on AsTher values:

$$\Delta H_f(T) = AT^5 + BT^4 + CT^3 + DT^2 + ET + F$$

Valid temperature range 298-1500 K

coefficients:

| | |
|---|---|
| A | -4.1638E-016 |
| B | 4.4247E-012 |
| C | -1.0196E-008 |
| D | -5.3339E-006 |
| E | 0.037074 |
| F | 64.532 |

| Specific heat capacity, $c_p$ [J/molK] | | | | | | | |
|---|---|---|---|---|---|---|---|
| C(s) | | | | | | | |
| T[K] | T[°C] | Muradov | NIST-JANAF[1] | Barin[1] | AsTher[1] | fit 1[1,2] | fit 2[2,3] |
| 298.15 | 25 | | 8.517 | 8.512 | 8.531 | 15.599 | 20.606 |
| 300 | 27 | | 8.581 | 8.594 | 8.604 | 15.607 | 20.607 |
| 350 | 77 | | 10.241 | | 10.417 | 15.826 | 20.620 |
| 400 | 127 | | 11.817 | 11.927 | 11.991 | 16.044 | 20.633 |
| 450 | 177 | | 13.289 | | 13.391 | 16.262 | 20.646 |
| 500 | 227 | | 14.623 | 14.633 | 14.649 | 16.481 | 20.659 |
| 550 | 277 | | | | 15.784 | 16.700 | 20.672 |
| 600 | 327 | | 16.844 | 16.884 | 16.809 | 16.918 | 20.685 |
| 650 | 377 | | | | 17.729 | 17.137 | 20.698 |
| 700 | 427 | | 18.537 | 18.59 | 18.55 | 17.355 | 20.711 |
| 750 | 477 | | | | 19.275 | 17.573 | 20.724 |
| 800 | 527 | | 19.827 | 19.827 | 19.906 | 17.792 | 20.737 |
| 850 | 577 | | | | 20.445 | 18.011 | 20.750 |
| 900 | 627 | | 20.824 | 20.792 | 20.893 | 18.229 | 20.763 |
| 950 | 677 | | | | 21.25 | 18.448 | 20.776 |
| 1000 | 727 | | 21.610 | 21.566 | 21.518 | 18.666 | 20.789 |
| 1050 | 777 | | | | 21.697 | 18.885 | 20.802 |
| 1100 | 827 | | 22.244 | 22.192 | 21.786 | 19.103 | 20.815 |
| 1123 | 850 | 22.5 | | | | 19.204 | 20.821 |
| 1150 | 877 | | | | 22.544 | 19.322 | 20.828 |
| 1173 | 900 | | | | | 19.423 | 20.834 |
| 1200 | 927 | | 22.766 | 22.702 | 22.76 | 19.540 | 20.841 |
| 1250 | 977 | | | | 22.954 | 19.759 | 20.854 |
| 1300 | 1027 | | 23.204 | 23.117 | 23.129 | 19.977 | 20.867 |
| 1350 | 1077 | | | | 23.287 | 20.196 | 20.880 |
| 1400 | 1127 | | 23.578 | 23.453 | 23.430 | 20.414 | 20.893 |
| 1450 | 1177 | | | | 23.561 | 20.633 | 20.906 |
| 1500 | 1227 | | 23.904 | 23.725 | 23.682 | 20.851 | 20.919 |

1 graphitic carbon

2 Flagan,R.; Seinfeld J. 1988. Fundamentals of Air Pollution Engineering. Prentice hall, USA

3 monatomic carbon

Fit based on AsTher values:

$$c_p(T) = AT^5 + BT^4 + CT^3 + DT^2 + ET + F$$

Valid temperature range 298-1500 K

coefficients:

| | |
|---|---|
| A | -1.2186E-014 |
| B | 4.9955E-011 |
| C | -6.4932E-008 |
| D | 1.0183E-005 |
| E | 0.042022 |
| F | -3.5096 |

| Specific heat capacity, $c_p$ [J/molK] | | | | | | |
|---|---|---|---|---|---|---|
| $CH_4$(g) | | | | | | |
| T [K] | T [°C] | Muradov | NIST-JANAF | Barin | AsTher | fit [1] |
| 298.15 | 25 | | 35.639 | 35.645 | 35.044 | 51.031 |
| 300 | 27 | | 35.708 | 35.707 | 35.148 | 51.073 |
| 350 | 77 | | 37.874 | | 38.013 | 52.210 |
| 400 | 127 | | 40.500 | 40.489 | 40.933 | 53.346 |
| 450 | 177 | | 43.374 | | 43.847 | 54.483 |
| 500 | 227 | | 46.342 | 46.349 | 46.721 | 55.619 |
| 550 | 277 | | | | 49.538 | 56.756 |
| 600 | 327 | | 52.227 | 52.232 | 52.287 | 57.892 |
| 650 | 377 | | | | 54.960 | 59.029 |
| 700 | 427 | | 57.794 | 57.798 | 57.553 | 60.165 |
| 750 | 477 | | | | 60.063 | 61.302 |
| 800 | 527 | | 62.932 | 62.929 | 62.488 | 62.438 |
| 850 | 577 | | | | 64.825 | 63.575 |
| 900 | 627 | | 67.601 | 67.591 | 67.075 | 64.711 |
| 950 | 677 | 70 | | | 69.236 | 65.848 |
| 1000 | 727 | | 71.795 | 71.782 | 71.308 | 66.984 |
| 1050 | 777 | | | | 73.290 | 68.121 |
| 1100 | 827 | | 75.529 | 75.523 | 75.181 | 69.257 |
| 1123 | 850 | | | | | 69.784 |
| 1150 | 877 | | | | 76.982 | 70.394 |
| 1173 | 900 | | | | | 70.920 |
| 1200 | 927 | | 78.833 | 78.839 | 78.692 | 71.530 |
| 1250 | 977 | | | | 80.311 | 72.667 |
| 1300 | 1027 | | 81.744 | 81.764 | 81.838 | 73.803 |
| 1350 | 1077 | | | | 83.275 | 74.940 |
| 1400 | 1127 | | 84.305 | 84.333 | 84.620 | 76.076 |
| 1450 | 1177 | | | | 85.873 | 77.213 |
| 1500 | 1227 | | 86.556 | 86.583 | 87.035 | 78.349 |

1 Flagan,R.; Seinfeld J. 1988. Fundamentals of Air Pollution Engineering. Prentice hall, USA

Fit based on AsTher values:

$$c_p(T) = AT^5 + BT^4 + CT^3 + DT^2 + ET + F$$

Valid temperature range 298-1500 K

coefficients:

| | |
|---|---|
| A | -6.8926E-015 |
| B | 3.5425E-011 |
| C | -7.1484E-008 |
| D | 5.2816E-005 |
| E | 0.042003 |
| F | 19.442 |

| **Sensible enthalpies[1], $H_{mt}$ [kJ/mol]** ($T_{ref}$ = 25°C) | | | | |
|---|---|---|---|---|
| **T [K]** | **T [°C]** | **$CH_4$** | **$H_2$** | **$N_2$** |
| 298.15 | 25 | 0.000 | 0.000 | 0.000 |
| 300 | 27 | 0.066 | 0.053 | 0.054 |
| 350 | 77 | 1.906 | 1.500 | 1.511 |
| 400 | 127 | 3.858 | 2.960 | 2.971 |
| 450 | 177 | 5.956 | 4.419 | 4.437 |
| 500 | 227 | 8.197 | 5.883 | 5.911 |
| 550 | 277 | 10.59 | 7.346 | 7.396 |
| 600 | 327 | 13.128 | 8.812 | 8.894 |
| 650 | 377 | 15.811 | 10.277 | 10.408 |
| 700 | 427 | 18.633 | 11.749 | 11.937 |
| 750 | 477 | 21.589 | 13.223 | 13.483 |
| 800 | 527 | 24.673 | 14.702 | 15.046 |
| 850 | 577 | 27.88 | 16.186 | 16.626 |
| 900 | 627 | 31.203 | 17.676 | 18.222 |
| 950 | 677 | 34.637 | 19.174 | 19.835 |
| 1000 | 727 | 38.175 | 20.679 | 21.463 |
| 1050 | 777 | 41.813 | 22.193 | 23.105 |
| 1100 | 827 | 45.544 | 23.717 | 24.760 |
| 1150 | 877 | 49.363 | 25.251 | 26.428 |
| 1200 | 927 | 53.266 | 26.796 | 28.109 |
| 1250 | 977 | 57.246 | 28.352 | 29.801 |
| 1300 | 1027 | 61.299 | 29.916 | 31.503 |
| 1350 | 1077 | 65.421 | 31.493 | 33.215 |
| 1400 | 1127 | 69.607 | 33.081 | 34.936 |
| 1450 | 1177 | 73.853 | 34.680 | 36.666 |
| 1500 | 1227 | 78.155 | 36.288 | 38.405 |

1 Raiko, R et al. 2002. Poltto ja palaminen. IFRF, Suomi

Fit based on tabulated values:

$$H_{mt}(T) = AT^5 + BT^4 + CT^3 + DT^2 + ET + F$$

Valid temperature range 298-1500 K

| coefficients: | $CH_4$ | $H_2$ | $N_2$ |
|---|---|---|---|
| A | 3.6100E-15 | -8.7727E-16 | 2.4909E-15 |
| B | -1.2785E-11 | 3.8542E-12 | -1.2304E-11 |
| C | 2.4632E-08 | -5.5542E-09 | 2.2659E-08 |
| D | 1.3556E-05 | 4.0624E-06 | -1.6369E-05 |
| E | 2.1921E-02 | 2.7696E-02 | 3.4278E-02 |
| F | -8.2583 | -8.5020 | -9.2767 |

**APPENDIX D – Photos of the material formed in the quartz tube**